NACA

RESEARCH MEMORANDUM

THE EFFECTS OF TIP-MOUNTED JET NACELLES

ON THE TRANSONIC CHARACTERISTICS

OF LOW-ASPECT-RATIO WINGS

By Charles F. Coe

Ames Aeronautical Laboratory
Moffett Field, Calif.

NATIONAL ADVISORY COMMITTEE
FOR AERONAUTICS

WASHINGTON

December 23, 1952

NATIONAL ADVISORY COMMITTEE FOR AERONAUTICS

RESEARCH MEMORANDUM

THE EFFECTS OF TIP-MOUNTED JET NACELLES

ON THE TRANSONIC CHARACTERISTICS

OF LOW-ASPECT-RATIO WINGS

By Charles F. Coe

SUMMARY

An investigation of the effects of tip-mounted jet-engine nacelles
on the aerodynamic characteristics of low-aspect-ratio rectangular and
tapered wings has been conducted using the transonic-bump technique.
The test Mach number was varied from 0.60 to 1.12 which corresponded to
a test Reynolds number range of 1.6 million to 2.1 million for the rect-
angular wings and 2.3 million to 3.1 million for the tapered wing.

Generally, the effect of the tip-mounted nacelles was to increase
the lift-curve slopes for the wings of aspect ratio 2 or greater with
upper or lower mounted nacelles causing larger increases than symmetri-
cally mounted nacelles. Significant increases in drag resulted from the
addition of the nacelles on all the airfoils. Although the drag increases
due to off-center nacelles were generally greater than the increases
resulting from symmetrically mounted nacelles, the drag due to lift of the
wings with off-center nacelles was less. Substantially greater increases
in drag were obtained for cambered airfoils when nacelles were mounted in
the upper position than when they were mounted in the lower position. A
slight destabilizing effect on all the airfoils resulted from the addition
of the nacelles.

INTRODUCTION

One of the problems arising from the development of aircraft to fly
at transonic and supersonic speeds is the selection of nacelle locations
for housing jet engines, armament, and fuel. Numerous investigations have
been made to show the relative merits of various nacelle locations on
swept and unswept wings of low and high aspect ratios. The large number
of variables involved, however, indicate a continued need for additional
testing.

The present tests were undertaken to investigate through the transonic speed range the effect of tip-mounted jet nacelles on the aerodynamic characteristics of low-aspect-ratio wings. The results include measurements of the lift, drag, and pitching moment of several rectangular wings with 63A-series sections and one tapered wing with a biconvex section. All the wings were tested with the nacelles mounted symmetrically and, in addition, some were tested with the nacelles mounted in positions below and above the tip.

<div align="center">SYMBOLS</div>

C_L lift coefficient $\left(\dfrac{\text{twice semispan lift}}{qS}\right)$

C_D drag coefficient $\left(\dfrac{\text{twice semispan drag}}{qS}\right)$

C_m pitching-moment coefficient, referred to $0.25\overline{c}$
        $\left(\dfrac{\text{twice semispan pitching moment}}{qS\overline{c}}\right)$

A aspect ratio $\left(\dfrac{b^2}{S}\right)$

M Mach number

M_L local Mach number

R Reynolds number based on mean aerodynamic chord

S total wing area (twice wing area of semispan model), square feet

V velocity, feet per second

b twice span of semispan model, feet

c local wing chord, feet

$\overline{c}$ mean aerodynamic chord $\left(\dfrac{\int_0^{b/2} c^2 dy}{\int_0^{b/2} c\, dy}\right)$, feet

q dynamic pressure $\left(\tfrac{1}{2}\rho V^2\right)$, pounds per square foot

y spanwise distance from plane of symmetry, feet

α angle of attack, degrees

ρ air density, slugs per cubic foot

C_{L_α} lift-curve slope measured at zero lift, per degree

$\dfrac{\partial C_D}{\partial C_L^2}$ drag due to lift, slope of curve of drag coefficient as a function of C_L^2

APPARATUS

Wind Tunnel and Equipment

These tests were conducted on the transonic bump in the Ames 16-foot high-speed wind tunnel. The bump is described in detail in reference 1. The aerodynamic forces and moments were measured by means of an electrical strain-gage balance mounted within the bump.

MODELS

The combinations of wings and nacelle locations investigated are presented in table I. The plan forms and dimensions of the models and typical jet-nacelle positions are shown in figures 1 and 2. A sketch of the nacelle with its ordinates is shown in figure 3.

The model nacelles were scaled from a nacelle 24.8 feet in length with a fineness ratio of 7.44 which was proportioned to house an axial-flow turbojet engine with an afterburner. A scale factor based on a 30,000-pound airplane with a wing loading of 60 pounds per square foot was used. Thus the dimensions of the nacelle varied with the size of the wing models.

In the symmetrical position, the nacelles were mounted at the wing tips with their center lines on the chordlines of the wings and in wing spanwise positions such that the wing spans were the same as those of the wings alone. In the lower and upper positions the nacelles were mounted with their center lines parallel to the wing chord line at the spanwise position of the symmetrically mounted nacelle. A wooden filler block separated the nacelle a minimum distance of 0.010 foot from the airfoil surface on all the rectangular wings of aspect ratio 2. Thus the variations in camber and thickness caused slight differences in the nacelle height above or below the wing chord line. Photographs showing typical nacelle arrangements and positions are shown in figure 4.

TESTS AND PROCEDURE

Range of Test Variables

The investigation was conducted over a Mach number range from 0.60 to 1.12. The variation of Reynolds number with Mach number for the rectangular and tapered wings is shown in figure 5. Angle of attack was varied from -6° to 30°. The maximum angle of attack for some of the wings was limited because of the bending stress at the root.

Reduction of Data

The test data have been reduced to standard NACA coefficient form. A tare correction to the drag of the models to account for the drag of the fence was evaluated by cutting the wing off flush with the fence and testing the fence alone. The tare corrections applied are given in table II. No attempt was made to evaluate or correct for interference effects of the fence on the wing or the effects of leakage around the fence.

A correction was applied to angle of attack and drag measurements to account for cross flow over the bump.

Faired plugs were installed on the nose and tail of a nacelle mounted in the symmetrical position on a rectangular wing in an effort to determine whether the internal flow was appreciably affecting the minimum drag. It was found that the minimum drag with the nacelle plugged was the same as that obtained with air flowing through the nacelle for all Mach numbers of the test.

The models mounted on the transonic bump are in a local high-velocity region. Typical contours of local Mach number in the bump flow field are shown in figure 6. Outlines of the wings have been superimposed on these diagrams to indicate the Mach number gradients which exist across the wings during the tests. No attempt has been made to evaluate the effects of these gradients. The test Mach numbers presented in this report are the average Mach numbers over the wings alone.

RESULTS AND DISCUSSION

All the wings and wing-nacelle combinations were tested without a fuselage. The presence of a fuselage may alter somewhat the effects of the nacelles at transonic speeds due to a shock pattern that would be

produced; however, the degree of influence of the shock pattern on the effects of the nacelles would be dependent on the fuselage shape.

Rectangular Wings

Basic data.- The lift, drag, and pitching-moment characteristics of the rectangular wing of aspect ratio 2 having a 63A004 airfoil section are shown in figure 7. These data are given for the wing alone and the wing plus the nacelle in the symmetrical position to show typical examples of the basic data from which the summary data presented in this paper were extracted. The summary plots are presented in this report with Mach number as the independent variable. This method of presentation was chosen to reduce the volume of data and still present the aerodynamic characteristics of most interest. The complete basic data and summary data for all the rectangular wings without the nacelles except the wings of aspect ratio 1.5 with symmetrical sections are given in references 2 and 3. Additional summary data for rectangular wings with symmetrical sections including data for the wings of aspect ratio 1.5 can be found in reference 4.

Lift-curve slopes.- The variation of lift-curve slope with Mach number for the rectangular wings is shown in figure 8. The values of lift-curve slopes presented have been measured at a lift coefficient of zero. Although slight nonlinearities may exist in the lift curves of the wings of lower aspect ratios (references 2, 3, and 4), the value of zero lift coefficient was considered most suitable as a basis for slope comparisons.

For wings of aspect ratio 1 and 1.5 having NACA 63A002 and 63A004 airfoil sections, the effect of adding the symmetrically mounted nacelle appeared practically negligible throughout the Mach number range (figs. 8(a), 8(b), 8(c), and 8(d)). Adding the symmetrically mounted nacelles to the cambered airfoils generally appeared to decrease the lift-curve slope slightly for wings with a thickness ratio of 2 percent and to increase the slope for wings with a thickness ratio of 4 percent. The variation of lift-curve slope with Mach number for the wing-nacelle combination was similar to that for the wing alone for the wings of aspect ratios 1 and 1.5.

Figures 8(e) and 8(f) indicate that for an aspect ratio of 2 the lift-curve slope was generally increased throughout the Mach number range by adding the nacelles in either the upper, lower, or symmetrical positions. An increase was also observed throughout the Mach number range for all the models with aspect ratios of 3 and 4 (figs. 8(g) and 8(h)). The largest increase in lift-curve slope, approximately 15 percent, occurred at Mach numbers above 1.0 for the 63A404 airfoil of aspect ratio 2 with the nacelles in the lower position. While this increase

was observed for the thickest and most highly cambered airfoil, trends
due to thickness or camber were difficult to establish and appear inconse-
quential. The results indicate that of the three nacelle positions, add-
ing the nacelles in either the lower or upper position generally caused
the greatest increase in lift-curve slope.

Figure 9 shows the variation of the lift-curve slope with aspect
ratio for Mach numbers from 0.60 through 1.08 for the rectangular wings
with a 63A004 airfoil section. Data are given for the wing alone and
for the wing plus the nacelle in the symmetrical and lower positions.
The results indicate that at the lowest subsonic Mach number, the lift-
curve slope of the wing with or without the nacelles increased approxi-
mately linearly as the aspect ratio was increased from 1 to 4. At a
Mach number of 1.08 a more rapid increase in lift-curve slope occurred
at the lower aspect ratios than at the higher aspect ratios. The results
also indicate that for this airfoil at Mach numbers below 1 differences
in lift-curve slopes due to the nacelles were greatest at an aspect ratio
of about 3.5, while at Mach numbers above 1 these differences were great-
est at an aspect ratio near 2.

Drag.- The variation of drag coefficient with Mach number for the
rectangular wings is shown in figure 10 for lift coefficients of 0, 0.2,
and 0.4. Significant increases in drag were observed for all airfoils
when the nacelles were added. The incremental increases in drag coef-
ficient due to the addition of symmetrically mounted nacelles were rela-
tively unaffected by variations in wing thickness ratio or camber except
for those wings cambered for ideal lift coefficients of 0.4. Drag
increases due to the nacelles were from 20 percent to 50 percent less at
all lift coefficients for the wings of aspect ratio 1, and at a lift
coefficient of 0.4 for the wings of aspect ratios 1.5 and 2.

For the uncambered airfoils of aspect ratio 2, it is apparent (see
figs. 10(m) through 10(r)) that of the three nacelle positions the
symmetrically mounted nacelle generally increased the drag the least and
the effects of the lower and upper mounted nacelles were nearly alike.
For the cambered airfoils of aspect ratio 2, the effects of the lower
and symmetrically mounted nacelles were nearly alike and were substan-
tially less than those of the upper nacelle. The fact that the off-
center positions both result in higher drags than the centrally mounted
nacelle at Mach numbers above drag divergence is probably due to a large
extent to the thickness of the filler block used on these models between
the wing and the nacelle. The increased frontal area of the filler blocks
may also be partially responsible for higher drags of the off-center
nacelles throughout the Mach number range. Since the drag increases
caused by the lower nacelles mounted on the cambered airfoils were only
slightly different than those for the symmetrical position, it is possible,
through cleaner nacelle installations on larger-scale models, that the
drag increases due to a lower nacelle may be no greater than those due to
a centrally mounted nacelle.

Drag due to lift.- The variation with Mach number of a drag-due-to-lift parameter $(\partial C_D/\partial C_L^2)$ is shown in figure 11. The parameter is the slope of the linear portion of the curve of drag coefficient plotted as a function of list coefficient squared. The linearity range of the curves extended from about $C_L = 0.2$ to $C_L = 0.5$. The parameter is presented as a further indication of the effects of the three nacelle positions on the drag characteristics of the rectangular wings. With two exceptions (fig. 11(f)), the drag due to lift of the wing plus the nacelle in the symmetrical position was higher than that for the wing alone. Where these exceptions occur, the differences are relatively small and probably within the limits of accuracy of the data. On the other hand, for aspect ratios 1, 2, and 4, the drag due to lift of the wing plus the off-center nacelles was always less, regardless of Mach number, than that resulting from the symmetrical nacelles. In several cases of cambered wings with off-center nacelles (figs. 11(e) and 11(f)) drag due to lift was less than that for the wing alone. Generally, it appears that the upper nacelle position resulted in the least drag due to lift except at higher Mach numbers for the wings with thickness ratios of 4 percent. The differences in the effects of the upper and lower nacelles in some cases are not systematic, however, and are probably of little significance.

Pitching moment.- The pitching-moment characteristics of the rectangular wings and wing-nacelle combinations are presented in figure 12 for lift coefficients of 0, 0.2, and 0.4. Changes in pitching-moment coefficient due to the addition of the symmetrical nacelle were small at $C_L = 0$. The zero-lift pitching-moment characteristics of those airfoils to which the off-center nacelles were attached indicated a positive increment of pitching moment with the nacelle in the lower position and a negative increment with the nacelle in the upper position (figs. 12(d), 12(m), 12(n), 12(o), 12(p), 12(q), 12(r), and 12(t)). This is contrary to the effect that might be expected if the off-center nacelle drag were contributing appreciably to the changes in pitching moment. However, calculations show that the changes in pitching-moment coefficient would be almost insignificant, resulting from the drag increases if they were assumed acting through the center of the nacelles. Apparently, then, this effect of the off-center nacelles on the pitching moment at zero-lift coefficient is caused by flow interference in the region of the wing tip.

Some decrease in stability due to the symmetrically mounted nacelle is indicated throughout the Mach number range by the increase in the difference between the pitching-moment curves with and without the nacelle with increasing lift. The destabilizing effect appears to diminish with increase in aspect ratio and becomes of little significance for aspect ratios of 3 and 4. Effects on the stability of wings of aspect ratio 2 due to the off-center nacelles were about the same as the effects resulting from the symmetrically mounted nacelle. The transonic changes in pitching-moment characteristics of all the wing-nacelle combinations were generally similar to those of the wing alone.

Tapered Wing

The aerodynamic characteristics of the tapered wing with and without
the symmetrically mounted nacelle are shown in figure 13. The effects of
the symmetrical nacelle on the parameters C_{L_α} and $\partial C_D/\partial C_L^2$ are presented
as functions of Mach number in figure 14. The variation of drag coeffi-
cient and pitching-moment coefficient with Mach number at lift coefficients
of 0, 0.2, and 0.4 are presented in figures 15 and 16. The data show that
a slight increase in lift-curve slope occurred for all Mach numbers as a
result of the addition of the symmetrically mounted nacelle. The drag at
zero-lift coefficient was approximately doubled throughout the Mach number
range by adding the nacelle, and the incremental drag coefficient
increased with increasing lift coefficient. This fact was also indicated
by the higher drag due to lift $(\partial C_D/\partial C_L^2)$ which resulted from the addi-
tion of the nacelle (fig. 14). From the pitching-moment characteristics
(fig. 16), a destabilizing effect due to the symmetrical nacelle is indi-
cated that was small and relatively constant for all Mach numbers of the
test.

For all the parameters presented in this paper (except C_{L_α} at high
Mach numbers) there is close agreement between the effects of the nacelles
on the tapered wing and on the straight wing of the same aspect ratio,
camber, and thickness ratio (A = 2, 63A004).

CONCLUDING REMARKS

An experimental investigation of the longitudinal characteristics of
thin-wing-nacelle combinations having aspect ratios of 1 to 4 indicates
that for the Mach number range of 0.60 to 1.12 the general effect of the
nacelles was to increase the lift-curve slopes for the wings of aspect
ratio 2 or greater. Negligible effect was noted for the wings with aspect
ratios of 1 and 1.5. The symmetrically mounted wing-tip nacelles caused
smaller changes in the lift-curve slopes than the off-center nacelles.
Addition of the nacelles did not significantly affect the variation of
lift-curve slope with Mach number in the transonic Mach number range.

The addition of the nacelles resulted in significant increases in
drag for all the airfoils. The off-center nacelles generally caused
greater increases in drag than the symmetrically mounted nacelles at low
lift coefficients; however, the drag due to lift of the wings with off-
center nacelles was less. Substantially greater increases in drag were
obtained for the cambered airfoils when the nacelles were mounted in the
upper position than when they were mounted in the lower position.

The nacelles appeared to slightly reduce the longitudinal stability of all the airfoils. The effect of the nacelles on stability was about the same regardless of nacelle position.

Ames Aeronautical Laboratory
    National Advisory Committee for Aeronautics
        Moffett Field, Calif.

REFERENCES

1. Axelson, John A., and Taylor, Robert A.: Preliminary Investigation of the Transonic Characteristics of an NACA Submerged Inlet. NACA RM A50C13, 1950.

2. Nelson, Warren Howard, and McDevitt, John B.: The Transonic Characteristics of 17 Rectangular, Symmetrical Wing Models of Varying Aspect Ratio and Thickness. NACA RM A51A12, 1951.

3. Nelson, Warren Howard, and Krumm, Walter J.: The Transonic Characteristics of 38 Cambered Rectangular Wings of Varying Aspect Ratio and Thickness as Determined by the Transonic-Bump Technique. NACA RM A52D11, 1952.

4. McDevitt, John B.: A Correlation by Means of the Transonic Similarity Rules of the Experimentally Determined Characteristics of 22 Rectangular Wings of Symmetrical Profile. NACA RM A51L17b, 1952.

TABLE I.- WINGS AND NACELLE COMBINATIONS TESTED AND NACELLE LOCATIONS

Aspect ratio	Taper ratio	Wing section	Nacelle midlength location (percent c)	Nacelle positions tested indicated by height above or below wing chord line (percent c)		
				Symmetrical	Lower	Upper
1	1	63A002	0.5	0	----	----
↓	↓	63A202	↓	0	----	----
		63A402		0	----	----
		63A004		0	0.12	----
		63A204		0	----	----
↓	↓	63A404	↓	0	----	----
1.5	1	63A002	.4	0	----	----
		63A202		0	----	----
		63A402		0	----	----
		63A004		0	----	----
		63A204		0	----	----
↓	↓	63A404	↓	0	----	----
2	1	63A002	.4	0	.14	0.14
		63A202		0	.13	.15
		63A402		0	.13	.16
		63A004		0	.15	.15
		63A204		0	.14	.16
↓	↓	63A404	↓	0	.13	.17
3	1	63A004	.4	0	----	----
4	1	63A004	.4	0	.19	----
2	0.33	4-percent-thick circular arc	.5	0	----	----

TABLE II.- FENCE TARE-DRAG COEFFICIENTS

(a) Rectangular wing models, all Mach numbers tested

Aspect ratio	Fence tare-drag coefficient
1	0.0066
1.5	.0044
2	.0033
3	.0022
4	.0017

(b) Tapered wing model, Mach numbers as noted

Aspect ratio	Fence tare-drag coefficient
2 ↓	0.0050 M, 0.6 to 0.98 .0059 M, 1.02 .0066 M, 1.06 to 1.10

NOTE: Changes in angle of attack had negligible effect on fence tare-drag coefficients.

Aspect ratio

Leading edge

Fence

Symmetrical position

Upper position

Lower position
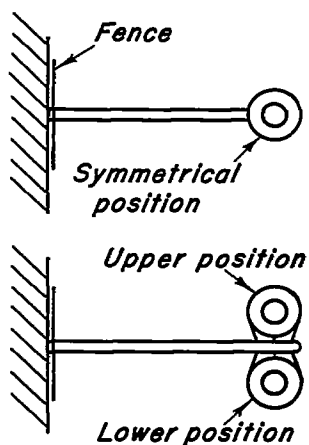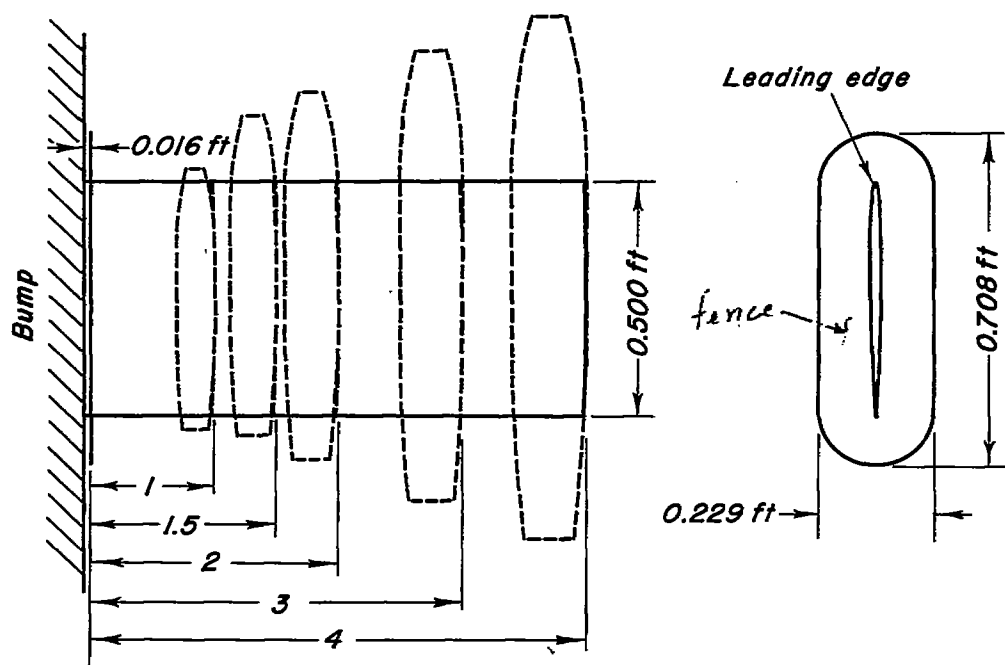
Aspect ratio	Semispan ft	Area of semispan sq ft	Nacelle length ft	Nacelle midlength location, %c
1	0.250	0.125	0.554	0.5
1.5	0.375	0.187	0.679	0.4
2	0.500	0.250	0.784	0.4
3	0.750	0.375	0.961	0.4
4	1.000	0.500	1.108	0.4

Figure l.-Plan forms and dimensions of the rectangular wings and typical nacelle positioning.

Figure 2.-Plan form and dimensions of the tapered wing and nacelle.

Aspect ratio	2
Taper ratio	0.333
Semispan area sq ft	0.444
Nacelle length ft	1.045

Note: All dimensions in feet.
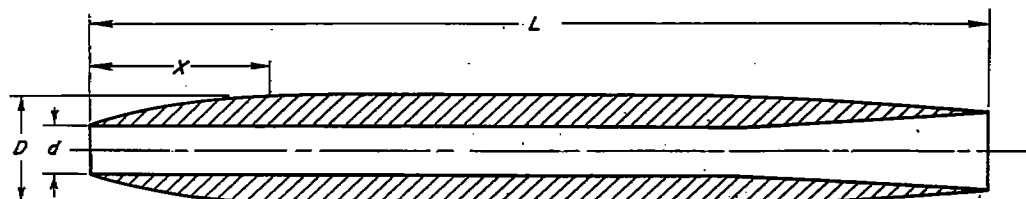
ORDINATES OF THE NACELLE

x Distance along center line	D Outside diameter	d Duct diameter
Percent L	Percent L	Percent L
0	5.90	5.71
1.64	7.20	5.71
3.39	8.07	5.71
5.03	8.85	5.71
10.07	10.76	5.71
13.45	11.72	5.71
16.84	12.41	5.71
20.14	12.76	5.71
25.17	13.37	5.71
29.43	13.45	5.71
40.00	13.45	5.71
50.00	13.45	5.71
60.00	13.45	5.71
63.02	13.45	5.71
68.92	13.28	5.71
72.31	12.93	
75.61	12.76	
78.99	12.41	
82.38	12.07	Linear taper
85.76	11.46	
89.06	11.02	
92.45	10.59	
95.83	9.98	
100.00	9.37	9.03

Figure 3.— Cross-sectional view and ordinates of the nacelle.
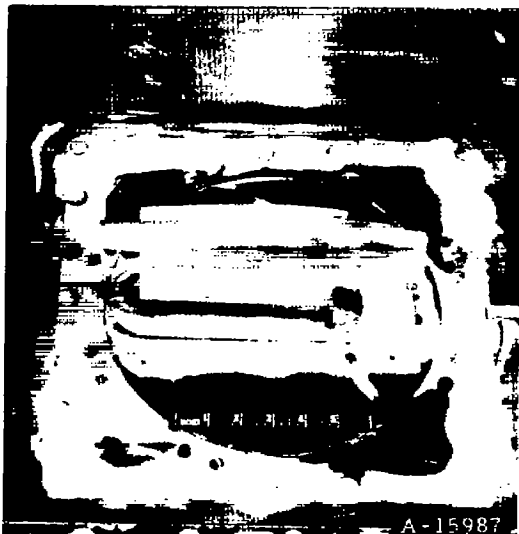
(a) Nacelle mounted in the
lower position.
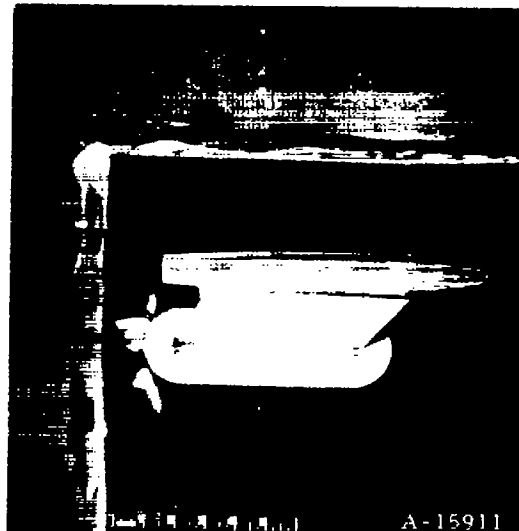
(b) Nacelle mounted in the
upper position.

(c) Nacelles mounted in the symmetrical position.
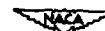
Figure 4.— Photographs of aspect ratio 2 wings with nacelles mounted in
the lower, upper, and symmetrical positions.
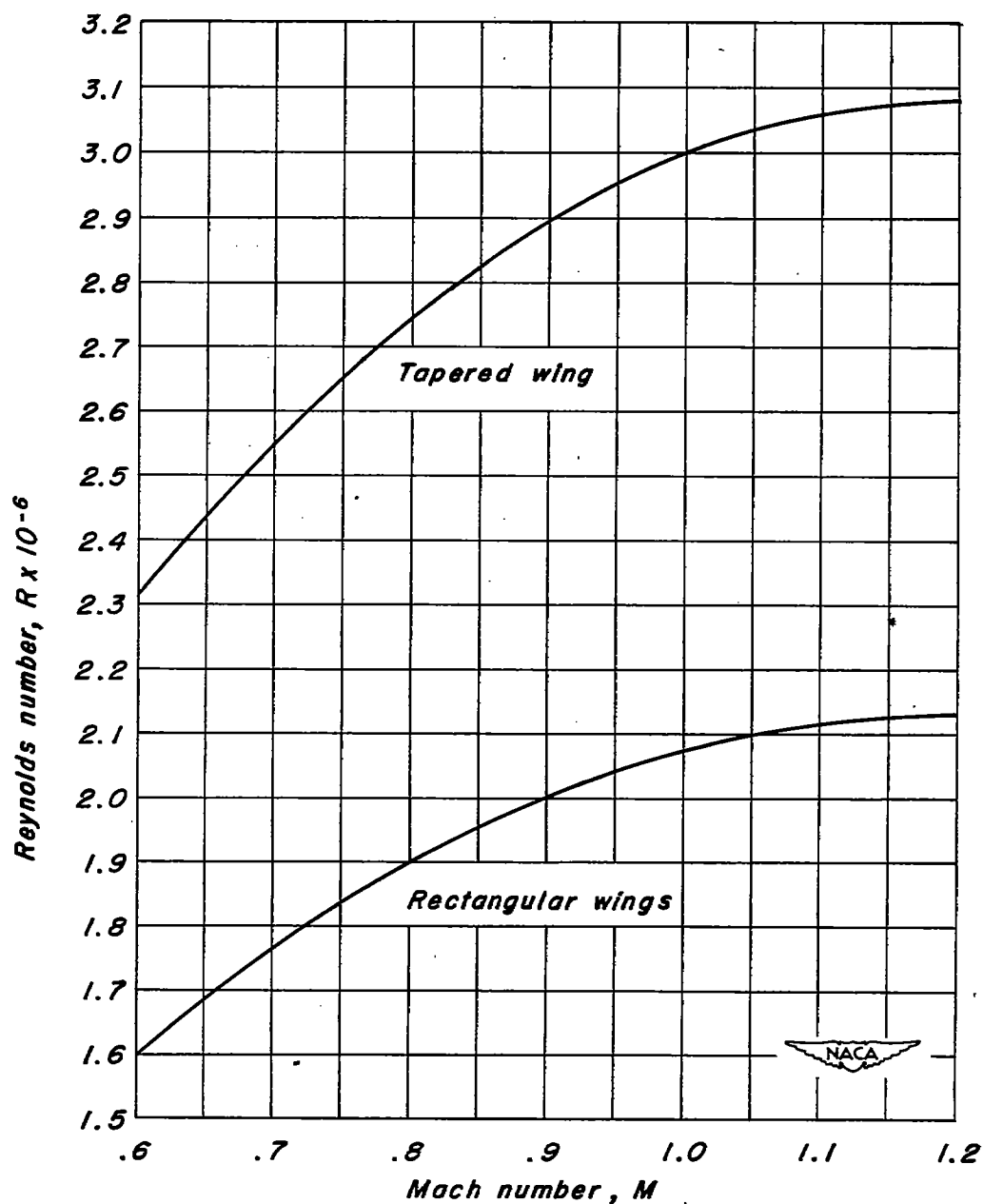
Figure 5.— The variation of Reynolds number with Mach number for the rectangular and the tapered wings.

(a) Rectangular wings.

Figure 6.- Typical Mach number contours over the transonic bump in the Ames 16-foot high-speed wind tunnel.
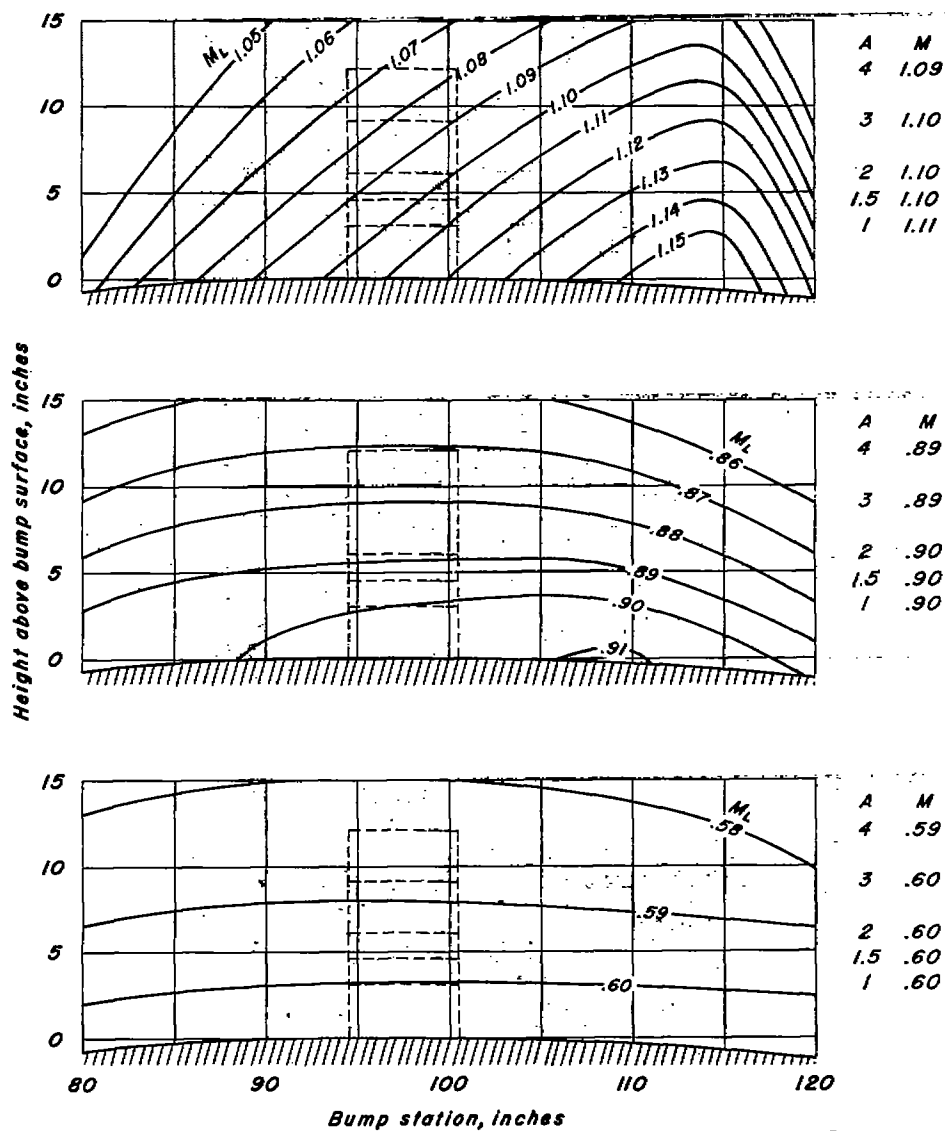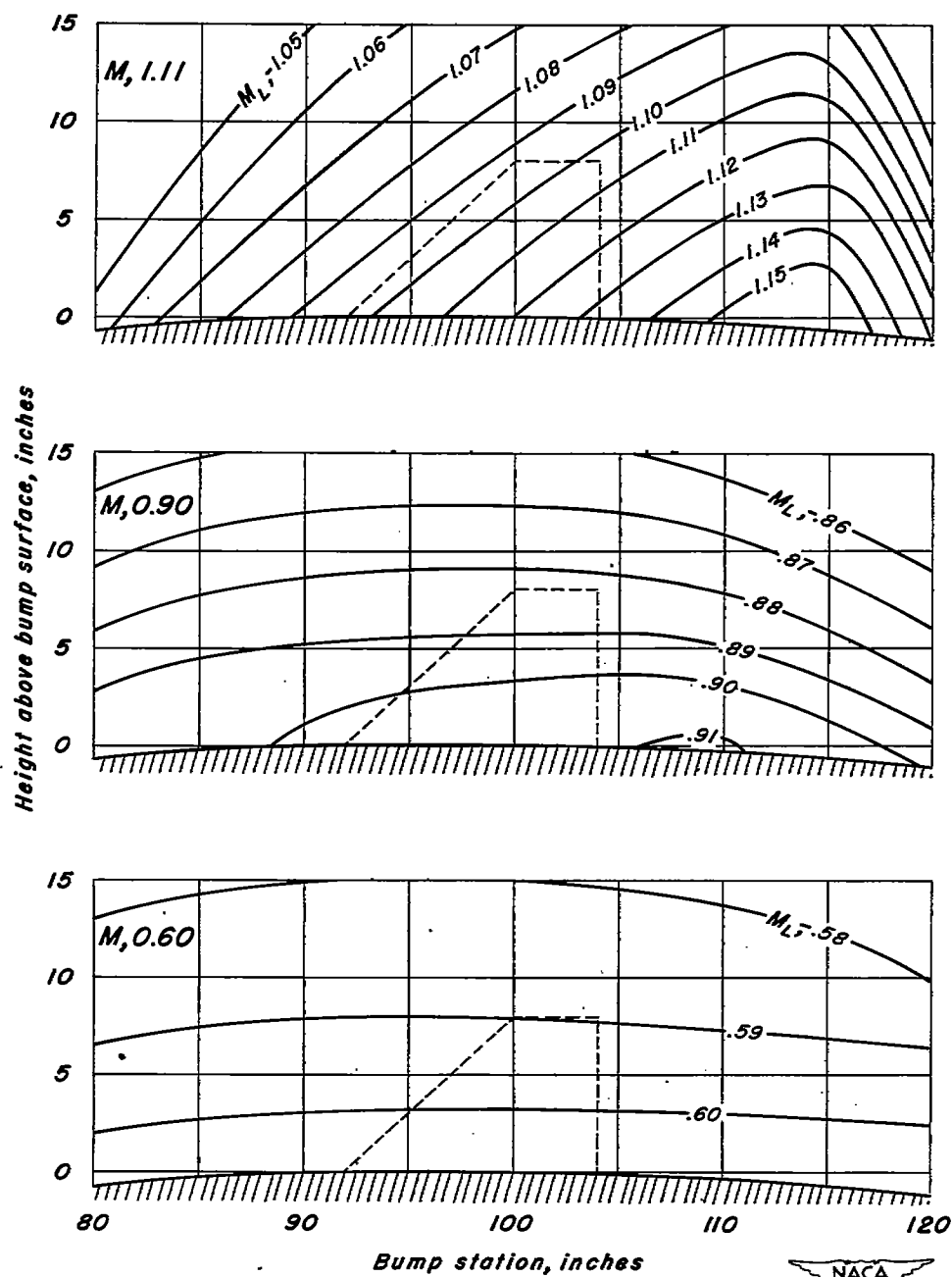
(b) Tapered wing

Figure 6.-Concluded.

(a) Wing alone.
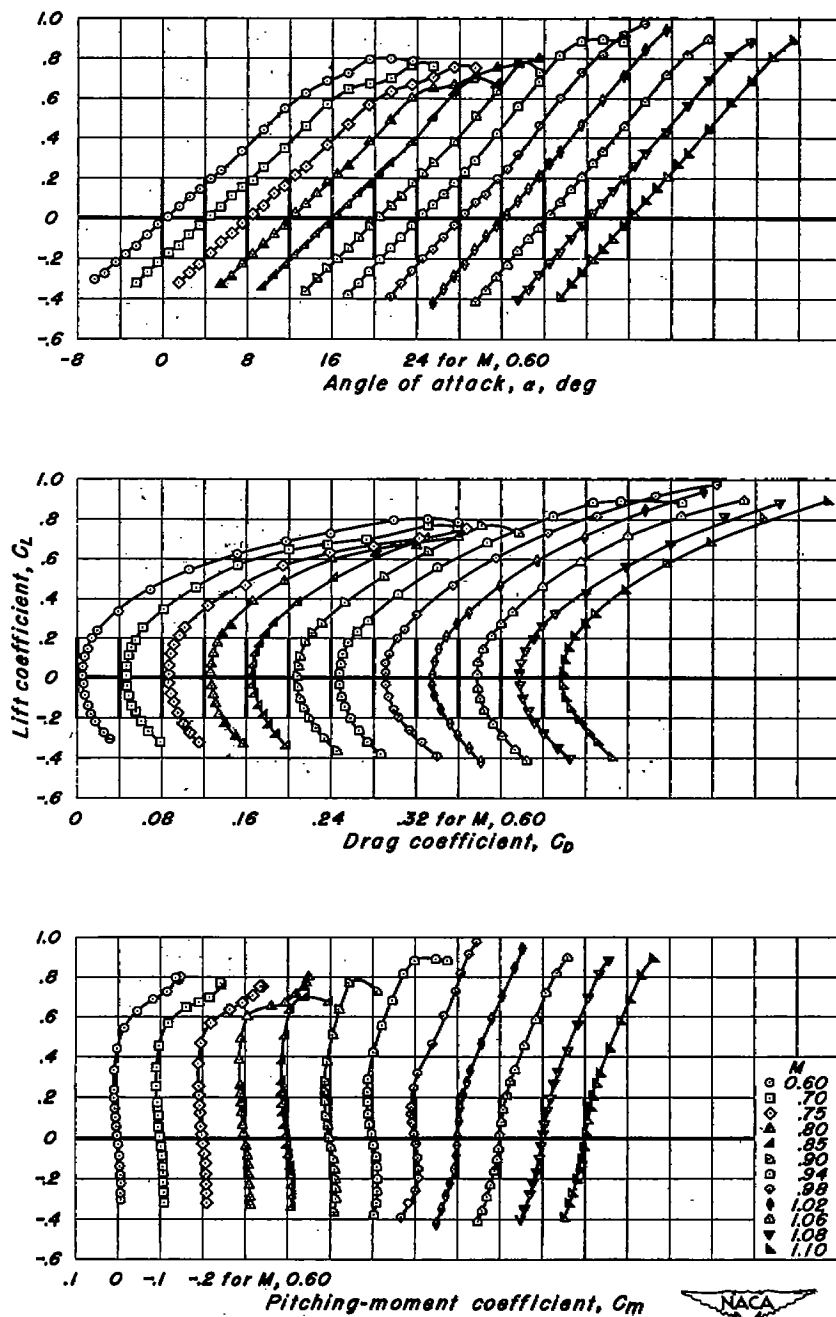
Figure 7.—The aerodynamic characteristics of the aspect ratio
2 rectangular wing with a 63A004 section.
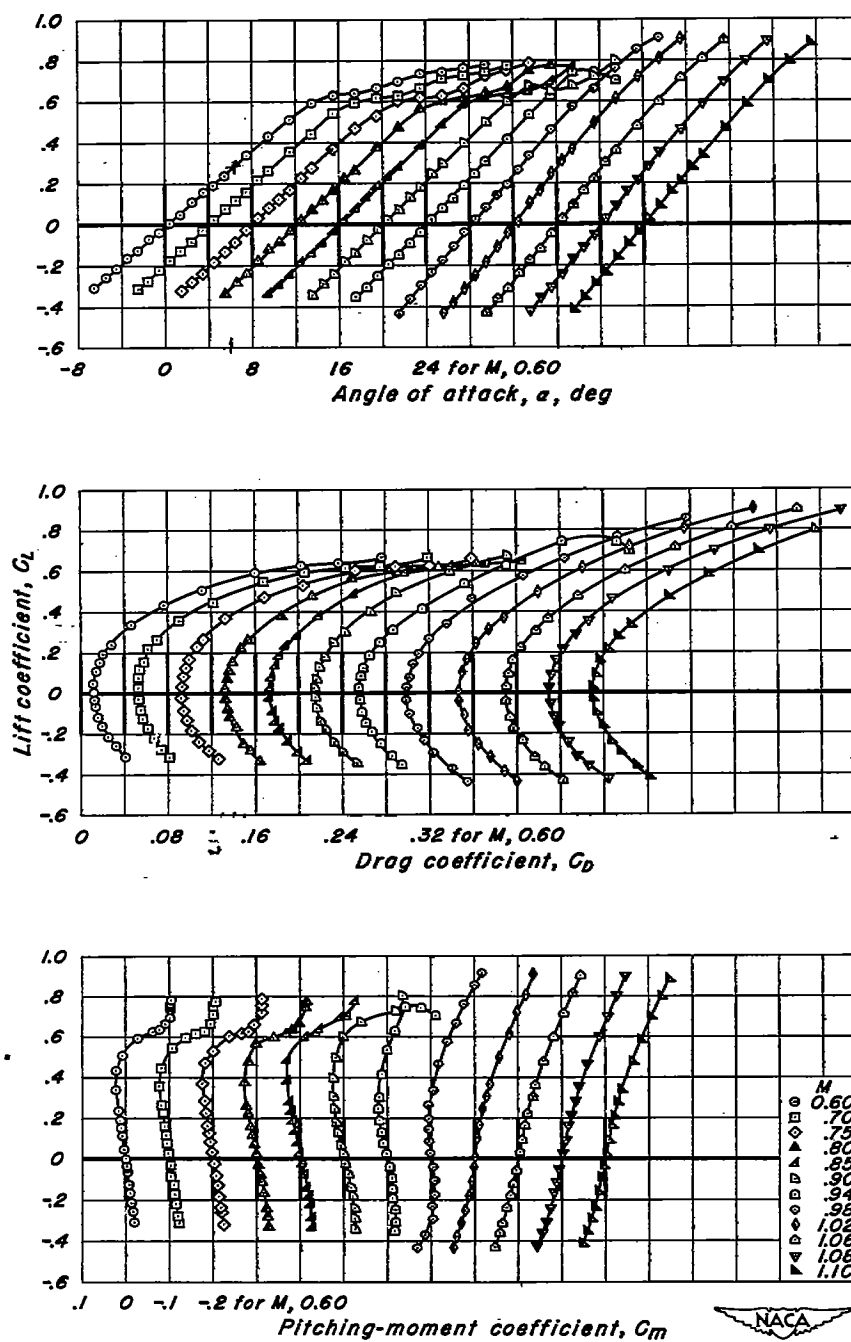
(b) Wing plus nacelle in symmetrical position.

Figure 7.— Concluded.

—————— Wing
———— —— Wing plus nacelle in symmetrical position
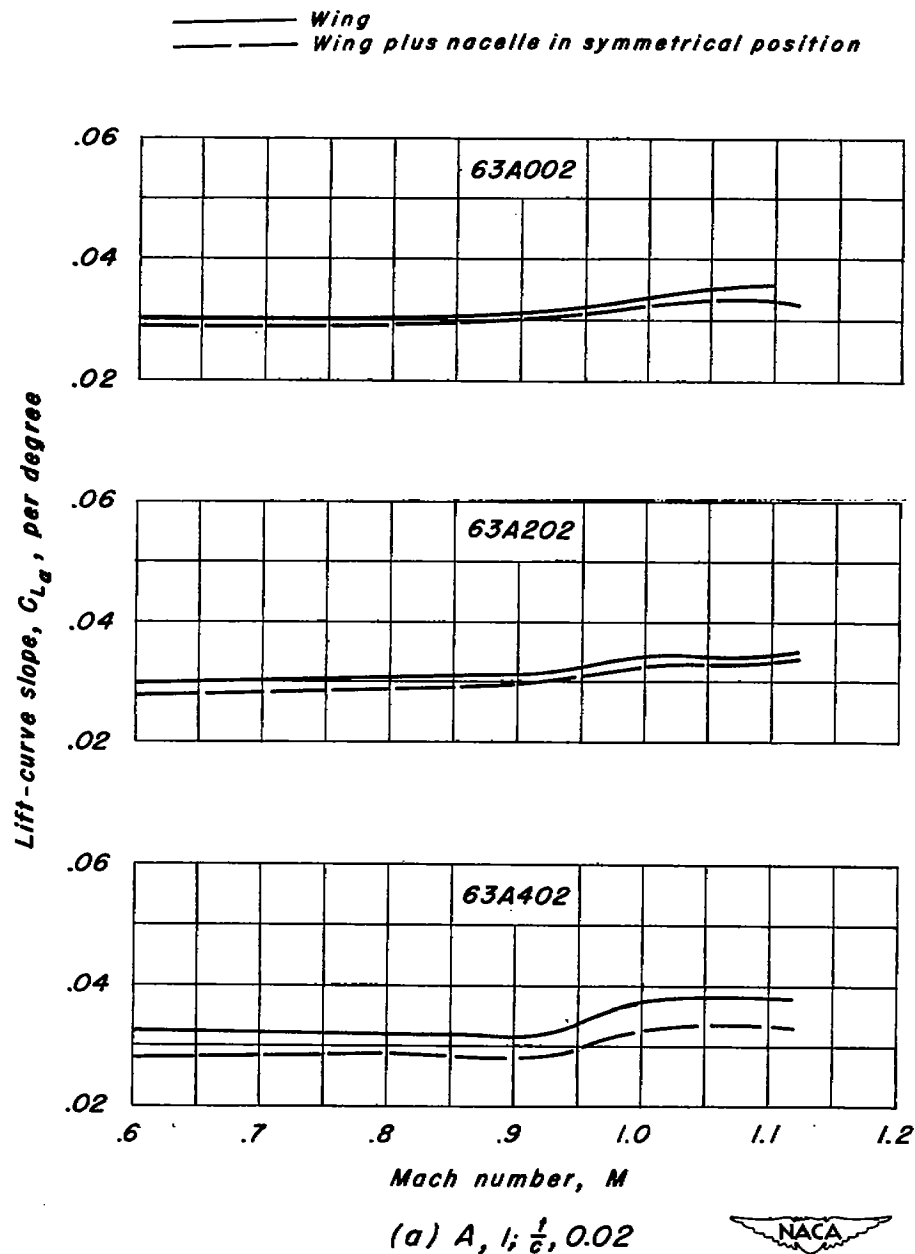
(a) A, 1; $\frac{t}{c}$, 0.02

Figure 8.—The variation of lift-curve slope with Mach number for the rectangular wings with NACA 63A series sections.

Wing
Wing plus nacelle in symmetrical position
Wing plus nacelle in lower position

(b) A, 1; $\frac{t}{c}$, 0.04

Figure 8.— Continued.

Wing
Wing plus nacelle in symmetrical position

(c) A, 1.5; $\frac{t}{c}$, 0.02

Figure 8.— Continued.

Wing
Wing plus nacelle in symmetrical position

63A004

63A204

63A404

Lift-curve slope, C_{L_α}, per degree

Mach number, M
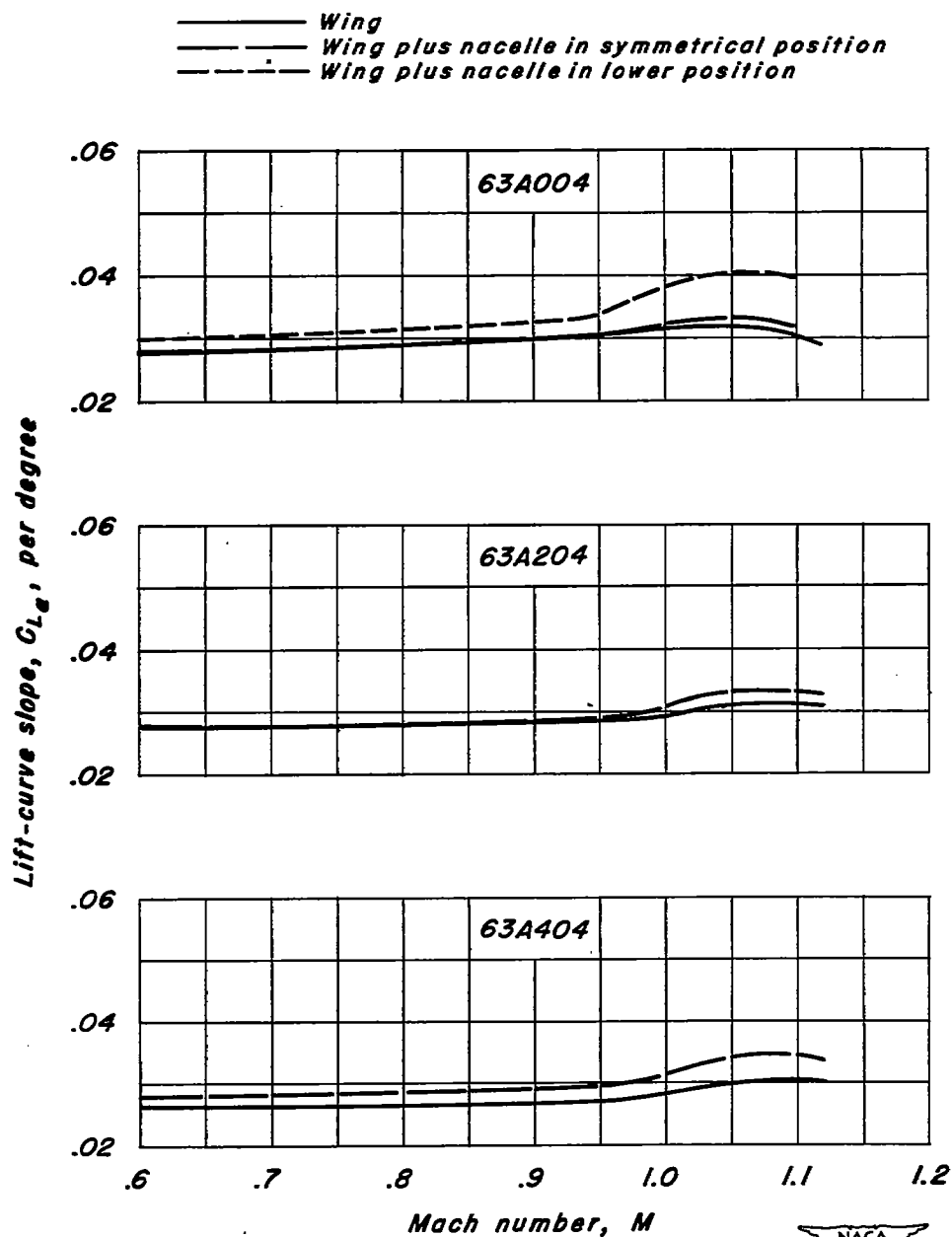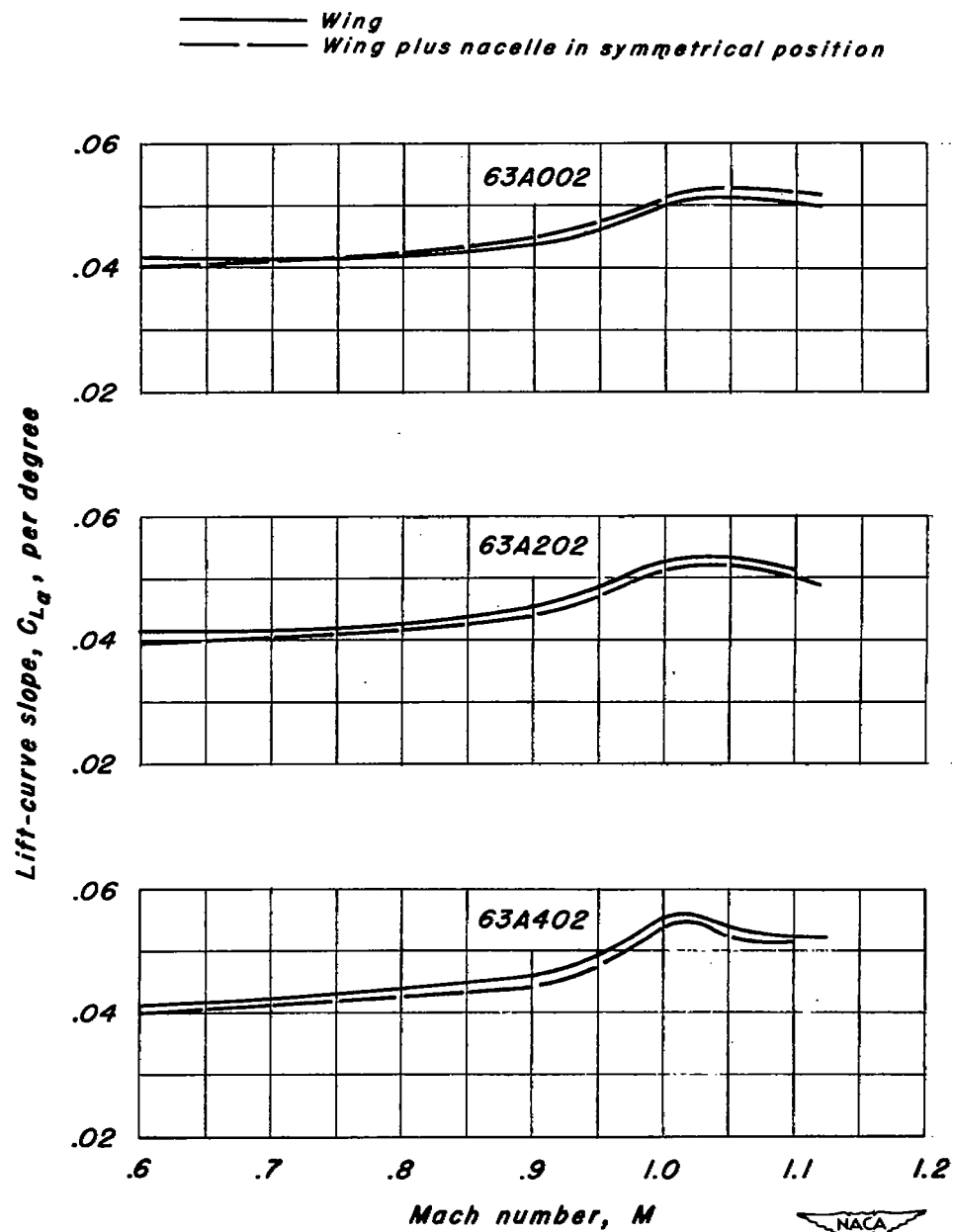
(d) A, 1.5; $\frac{t}{c}$, 0.04
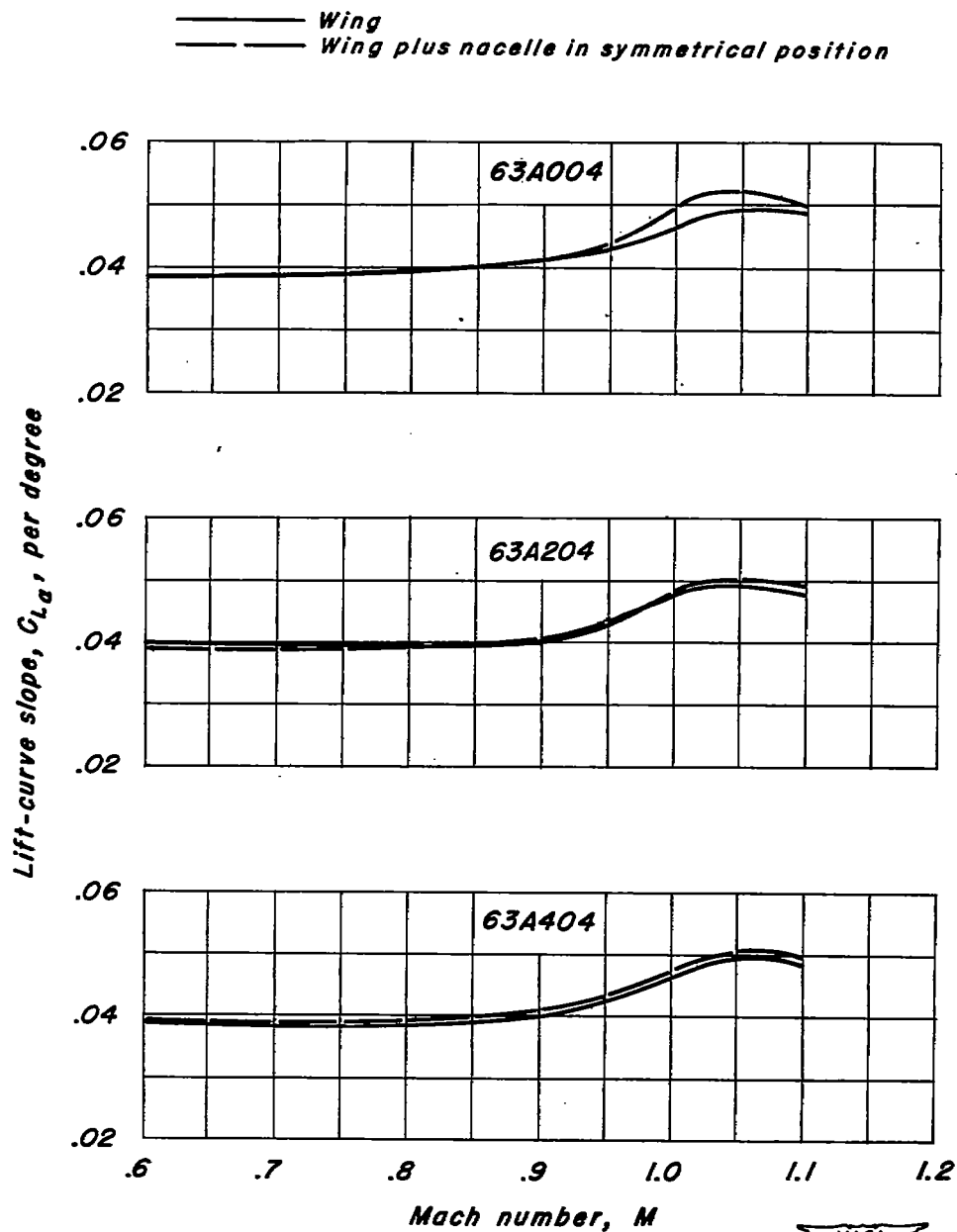
Figure 8.— Continued.

(e) A, 2; $\frac{t}{c}$, 0.02

Figure 8.—Continued.

Wing
Wing plus nacelle in symmetrical position
Wing plus nacelle in lower position
Wing plus nacelle in upper position
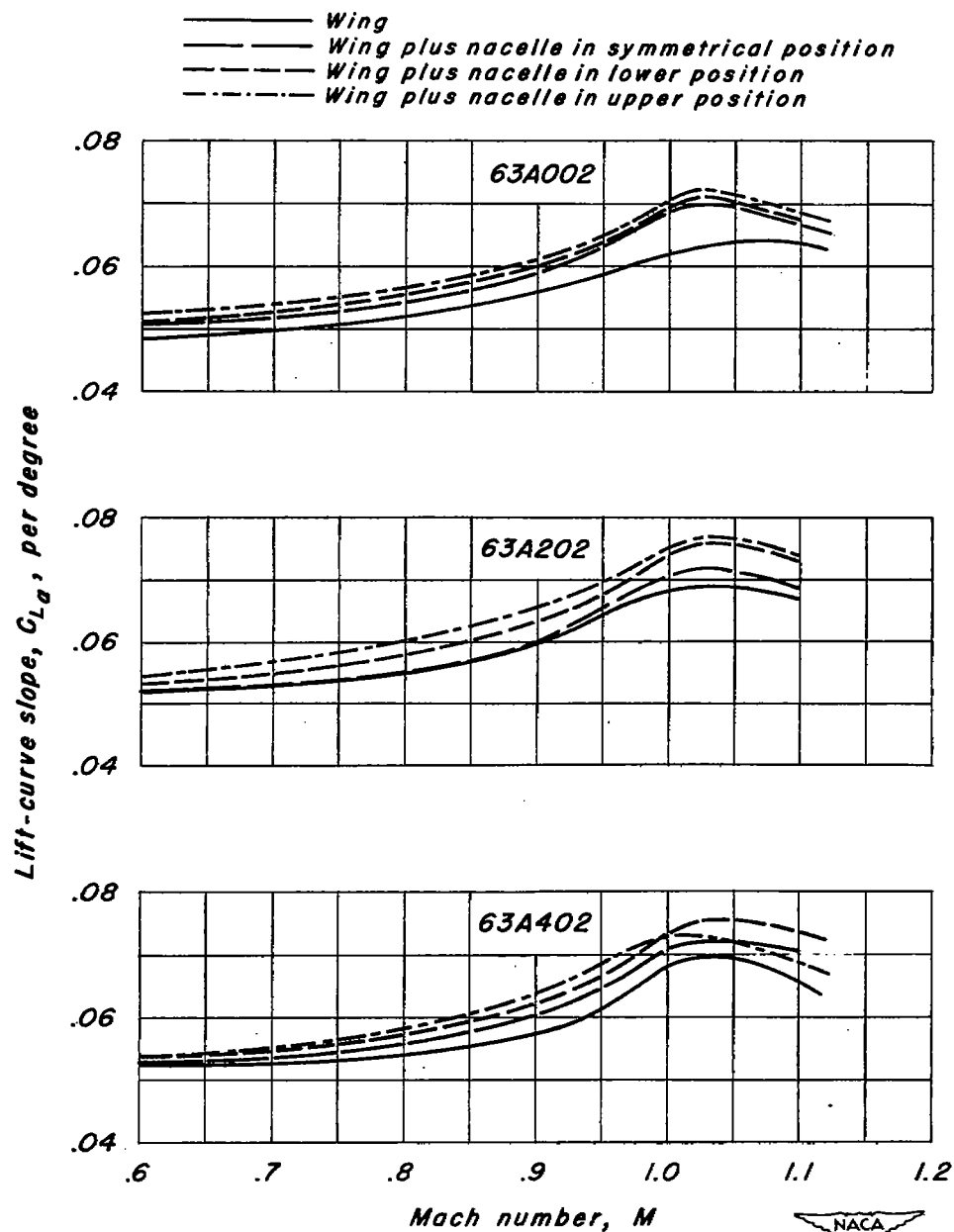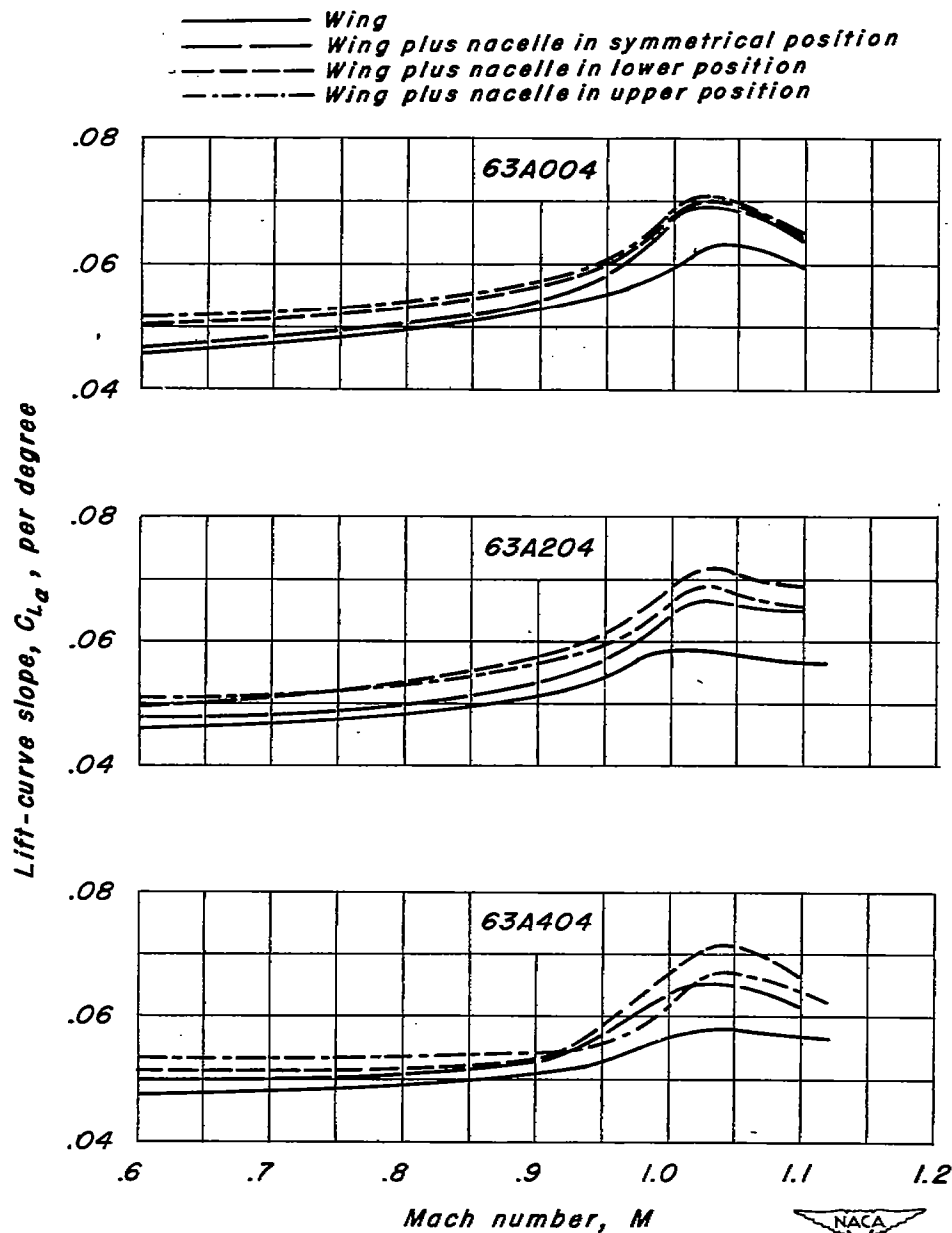
(f) A, 2; $\frac{t}{c}$, 0.04

Figure 8.-Continued.

—————— Wing
— · — Wing plus nacelle in symmetrical position
— — — — Wing plus nacelle in lower position
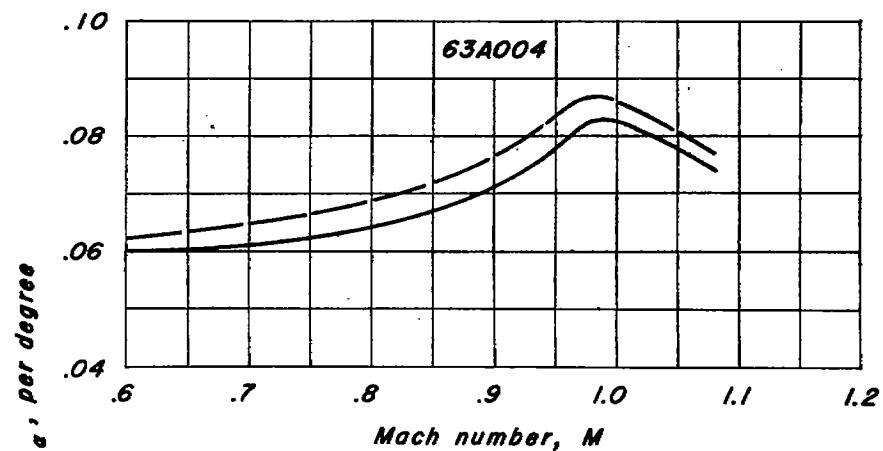
(g) A, 3; $\frac{t}{c}$, 0.04
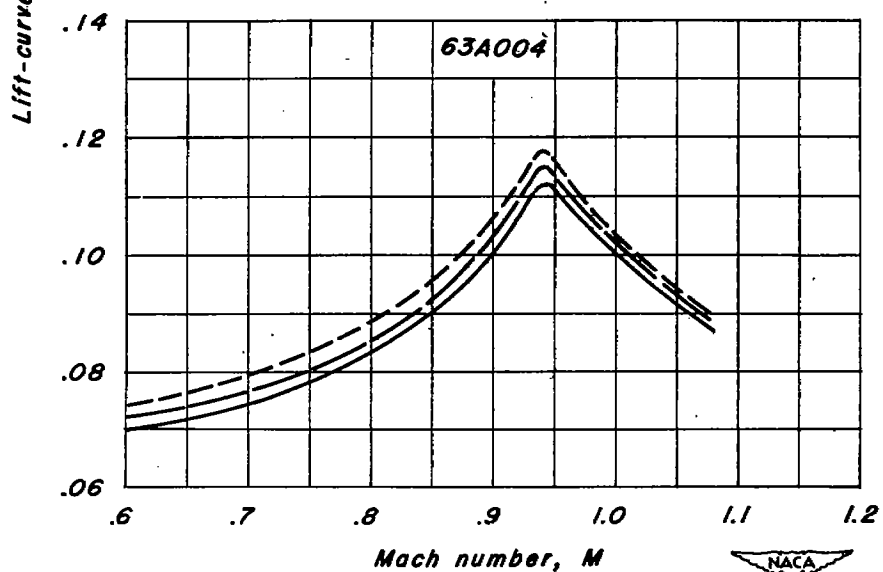
(h) A, 4; $\frac{t}{c}$, 0.04

Figure 8.—Concluded.
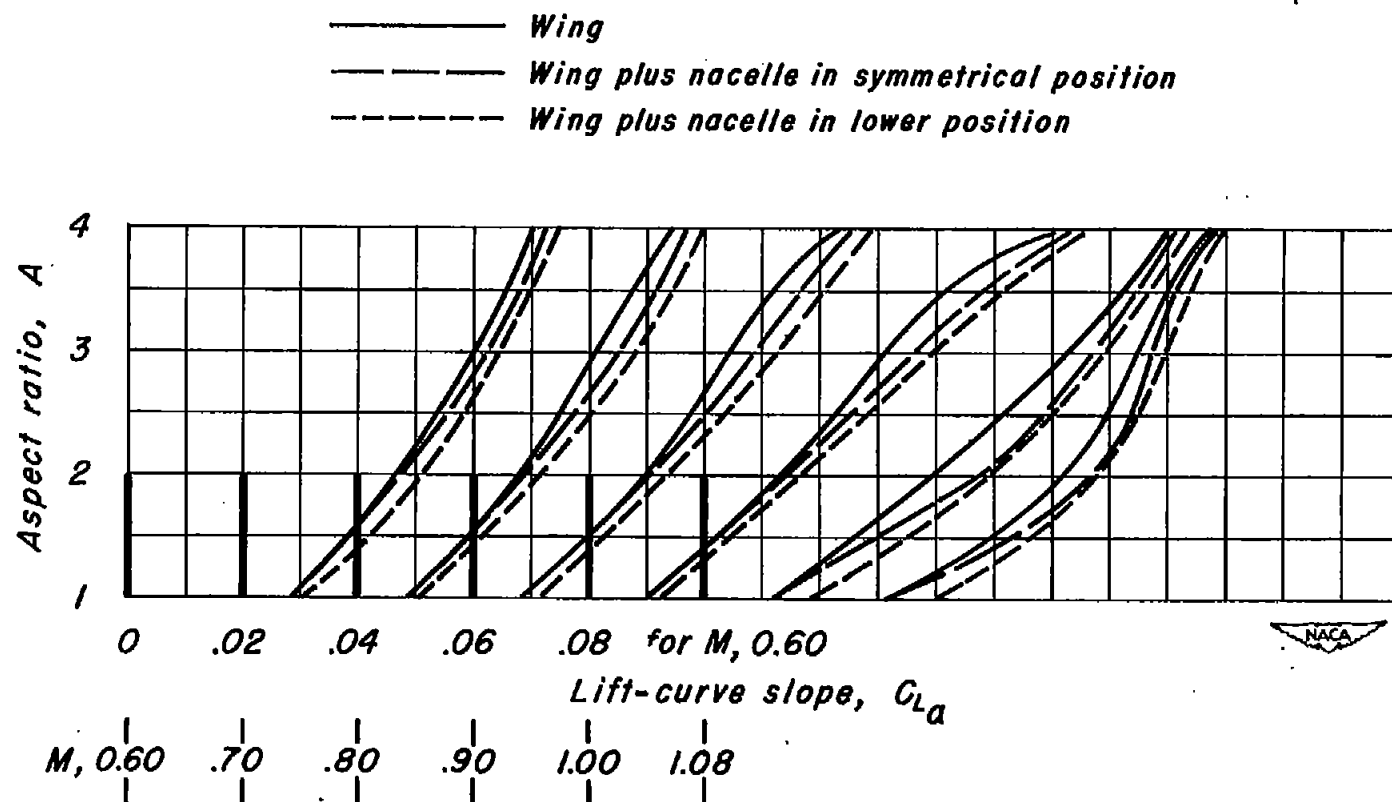
Figure 9.—The variation of lift-curve slope with aspect ratio for the rectangular wings with 63A004 sections.

——————— Wing
——— ——— Wing plus nacelle in symmetrical position
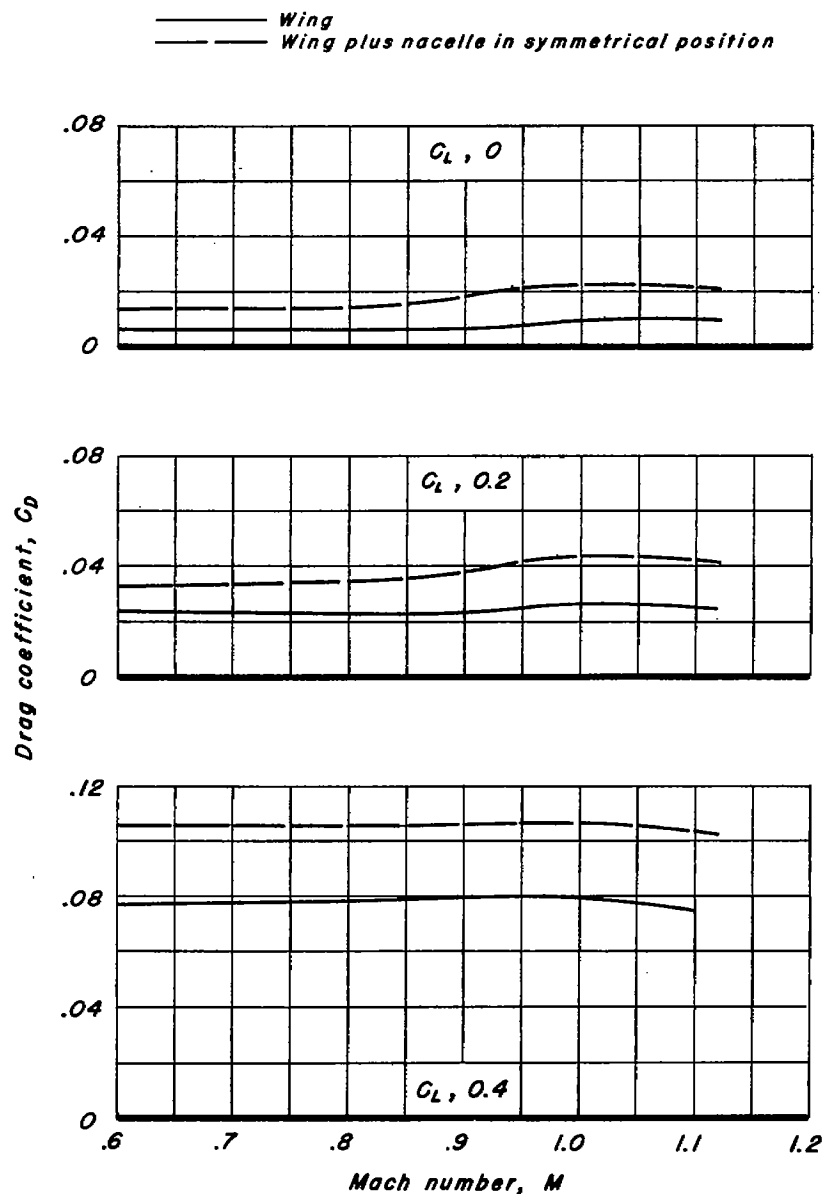
(a) A, 1; 63A002

Figure 10.— The variation of drag coefficient with Mach
number for the rectangular wings with NACA 63A
series sections.

——————— Wing
——— ——— Wing plus nacelle in symmetrical position

(b) A, I ; 63A202

Figure 10.—Continued.

Wing
Wing plus nacelle in symmetrical position

(c) A, 1 ; 63A402

Figure 10.—Continued.

Wing
Wing plus nacelle in symmetrical position
Wing plus nacelle in lower position

(d) A, 1; 63A004

Figure 10.—Continued.

——————— Wing
——·——·—— Wing plus nacelle in symmetrical position

C_L, 0

C_L, 0.2

C_L, 0.4

Drag coefficient, C_D

Mach number, M

(e) A, I ; 63A204

Figure 10.—Continued

Wing
Wing plus nacelle in symmetrical position

C_L , 0

C_L , 0.2

Drag coefficient, C_D

C_L , 0.4

Mach number, M

(f) A, l ; 63A404

Figure 10.—Continued.

(g) A, I.5; 63A002

Figure 10.—Continued.

——————— Wing
— — — — Wing plus nacelle in symmetrical position

(h) A, 1.5; 63A202

Figure 10.- Continued.

Wing
Wing plus nacelle in symmetrical position

C_L , 0

C_L , 0.2

C_L , 0.4

Drag coefficient, C_D

Mach number, M

(i) A, 1.5; 63A402

Figure 10.—Continued.

—————— Wing
— — —— Wing plus nacelle in symmetrical position

C_L , 0

.08

.04

0

C_L , 0.2

.08

Drag coefficient, C_D

.04

0

C_L , 0.4

.12

.08

.04

0

.6   .7   .8   .9   1.0   1.1   1.2

Mach number, M

(j) A, 1.5; 63A004

Figure 10.—Continued.

Wing
Wing plus nacelle in symmetrical position

C_L , 0

C_L , 0.2

Drag coefficient, C_D

C_L , 0.4

Mach number, M

(k) A, 1.5; 63A204

Figure 10.—Continued.

Wing
Wing plus nacelle in symmetrical position

(l) A, I.5; 63A404

Figure 10.—Continued.

Wing
——— Wing plus nacelle in symmetrical position
—·——— Wing plus nacelle in lower position
—·—·—·— Wing plus nacelle in upper position

C_L , 0

C_L , 0.2

Drag coefficient, C_D

C_L , 0.4

Mach number, M

(m) A, 2 ; 63A002

Figure 10.-Continued.

Wing
Wing plus nacelle in symmetrical position
Wing plus nacelle in lower position
Wing plus nacelle in upper position

(n) A, 2; 63A202

Figure 10.-Continued.

(o) A, 2 ; 63A402

Figure 10.—Continued.

Wing
—— —— Wing plus nacelle in symmetrical position
—— —— Wing plus nacelle in lower position
—··—··— Wing plus nacelle in upper position

(p) A,2; 63A004

Figure 10.— Continued.

Wing
Wing plus nacelle in symmetrical position
Wing plus nacelle in lower position
Wing plus nacelle in upper position

C_L, 0

C_L, 0.2

Drag coefficient, C_D

C_L, 0.4

Mach number, M

(q) A,2 ; 63A204

Figure 10.—Continued.

Wing
Wing plus nacelle in symmetrical position
Wing plus nacelle in lower position
Wing plus nacelle in upper position

C_L , 0

C_L , 0.2

C_L , 0.4

Drag coefficient, C_D

Mach number, M

(r) A, 2; 63A404

Figure 10.—Continued.

—————— Wing
— — — Wing plus nacelle in symmetrical position

C_L , 0

C_L , 0.2

Drag coefficient, C_D

C_L , 0.4

.6   .7   .8   .9   1.0   1.1   1.2

Mach number, M

NACA

(s) A,3; 63A004

Figure 10.—Continued.

—————— Wing
————— Wing plus nacelle in symmetrical position
— — — — Wing plus nacelle in lower position

(t) A, 4; 63A004

Figure 10.— Concluded.

——————— Wing
——— · ——— Wing plus nacelle in symmetrical position

63A002

63A202

63A402

Drag due to lift, $\frac{\partial C_{D_i}}{\partial C_L^2}$, per degree

Mach number, M

(a) A, I; $\frac{t}{c}$, 0.02
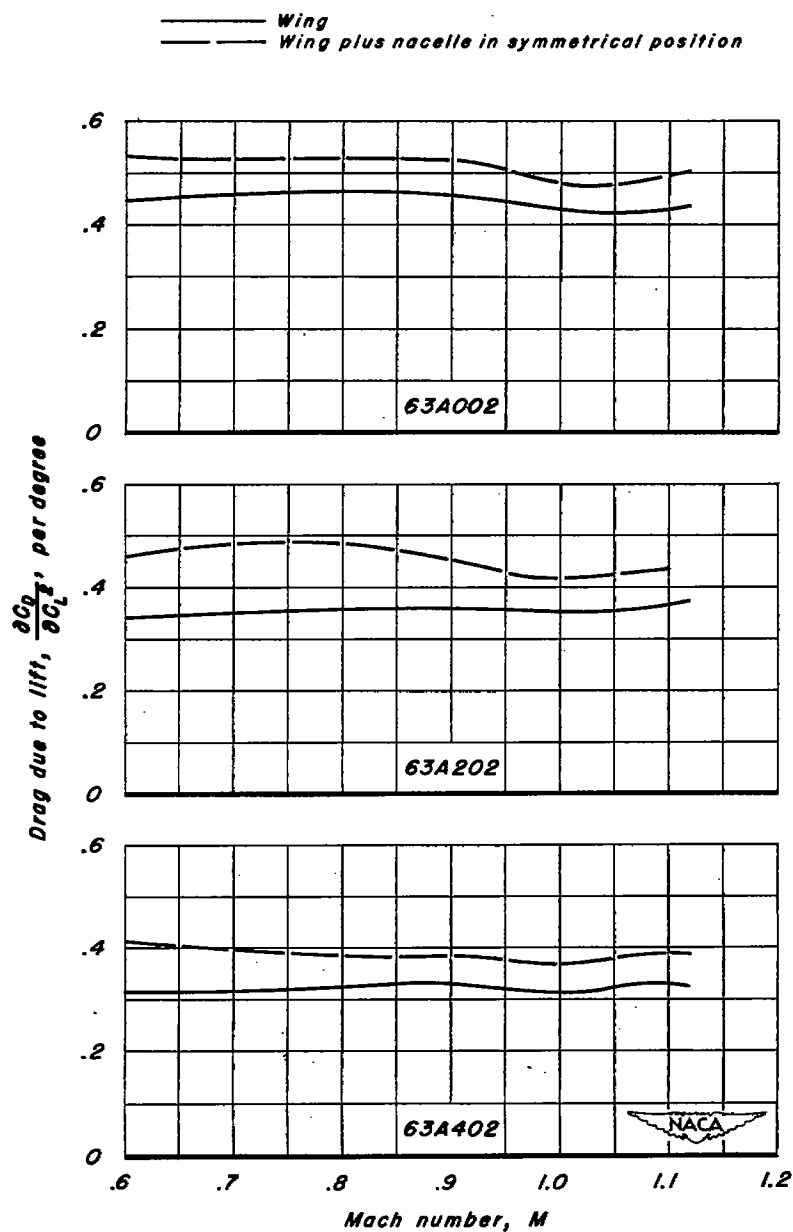
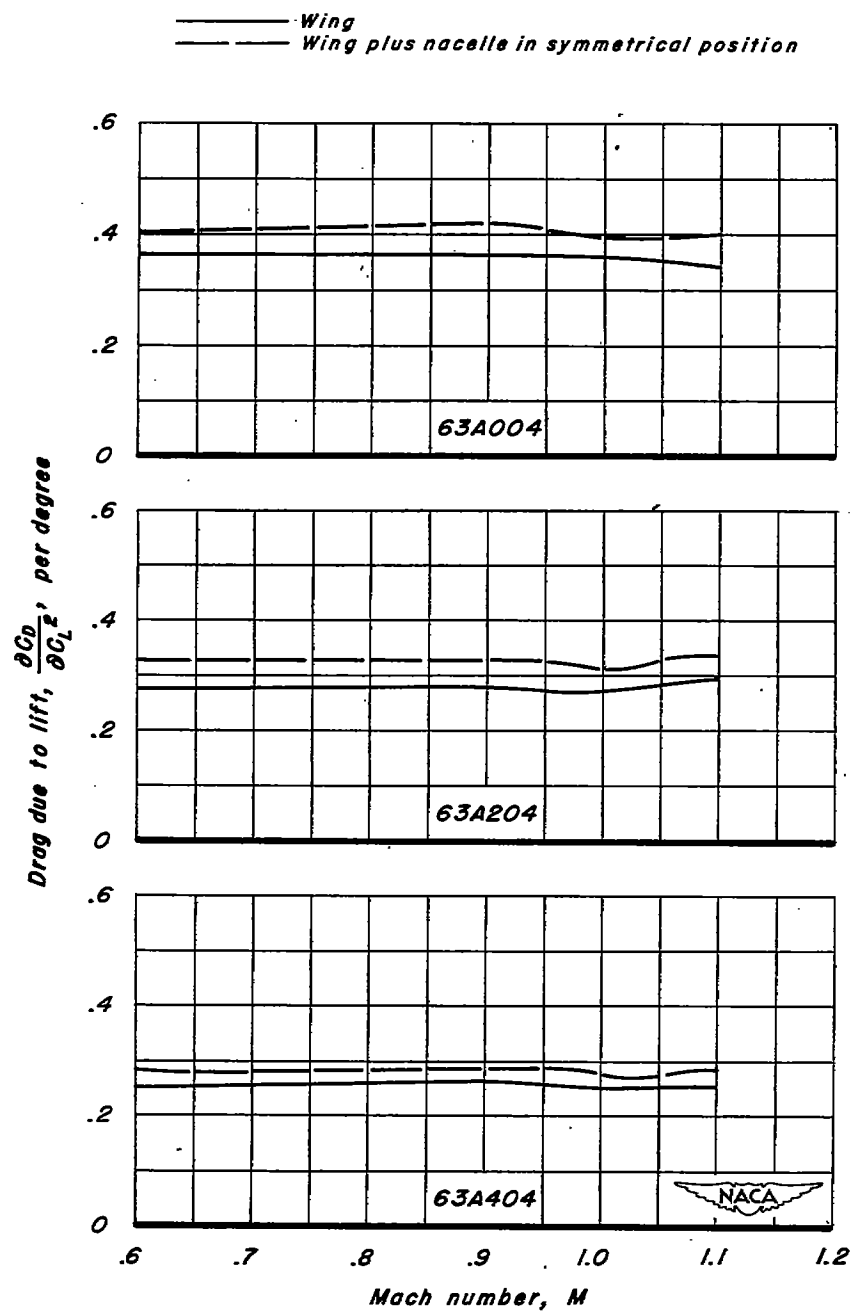Figure II.—The variation with Mach number of drag due to lift for the rectangular wings with 63A series sections.
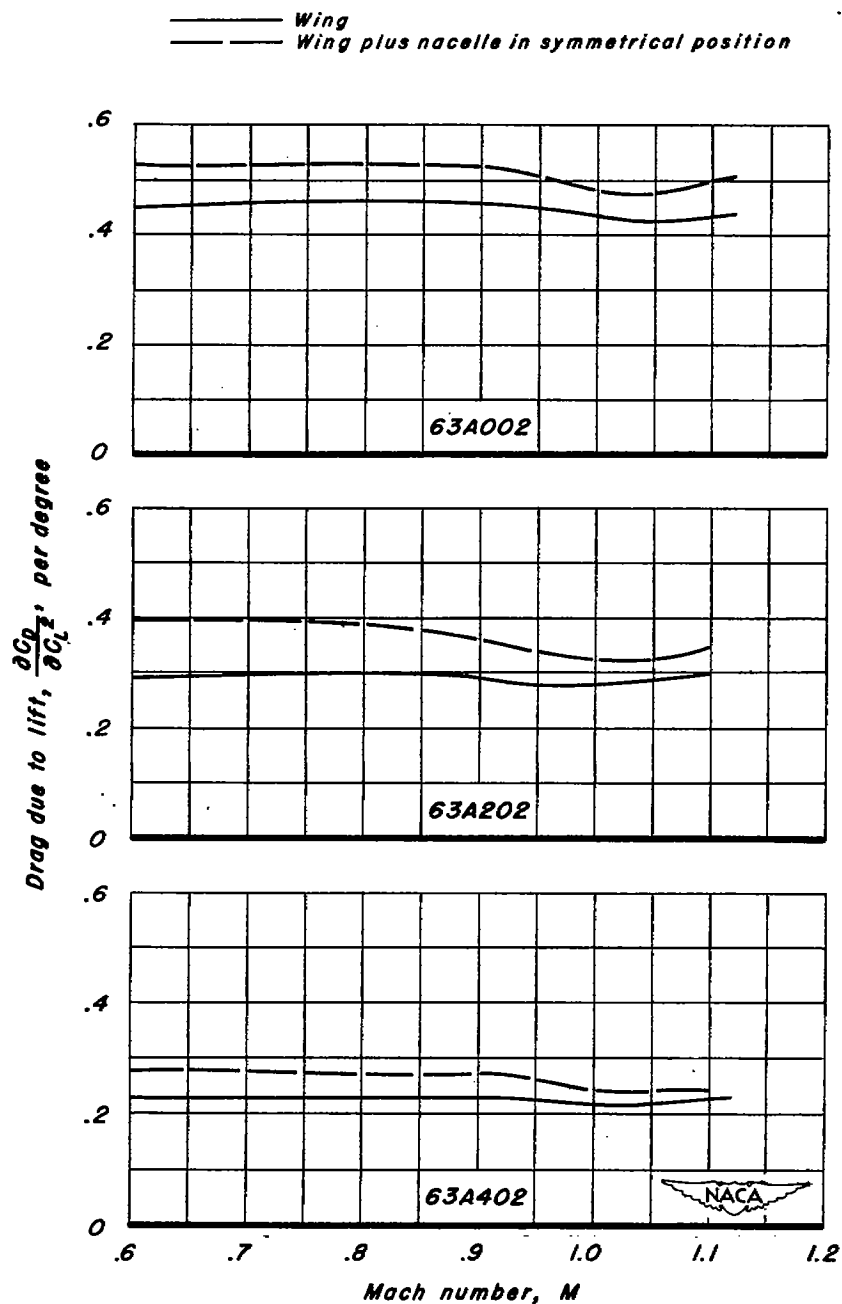
Wing
— — — Wing plus nacelle in symmetrical position
— — — — Wing plus nacelle in lower position

63A004

63A204

63A404

Mach number, M

(b) A, 1; $\frac{t}{c}$, 0.04

Figure 11.—Continued.

(c) $A, 1.5; \frac{t}{c}, 0.02$

Figure 11.— Continued.
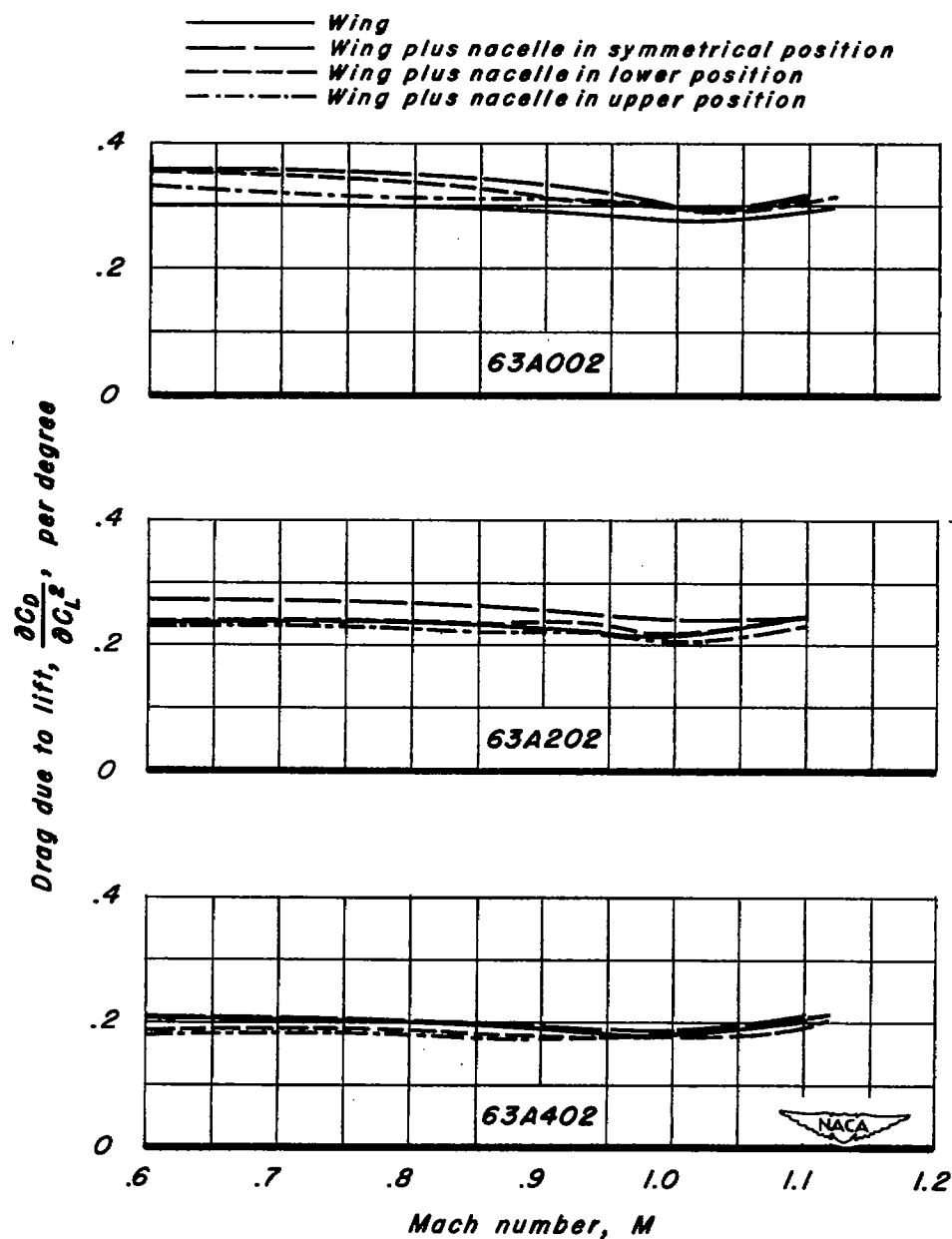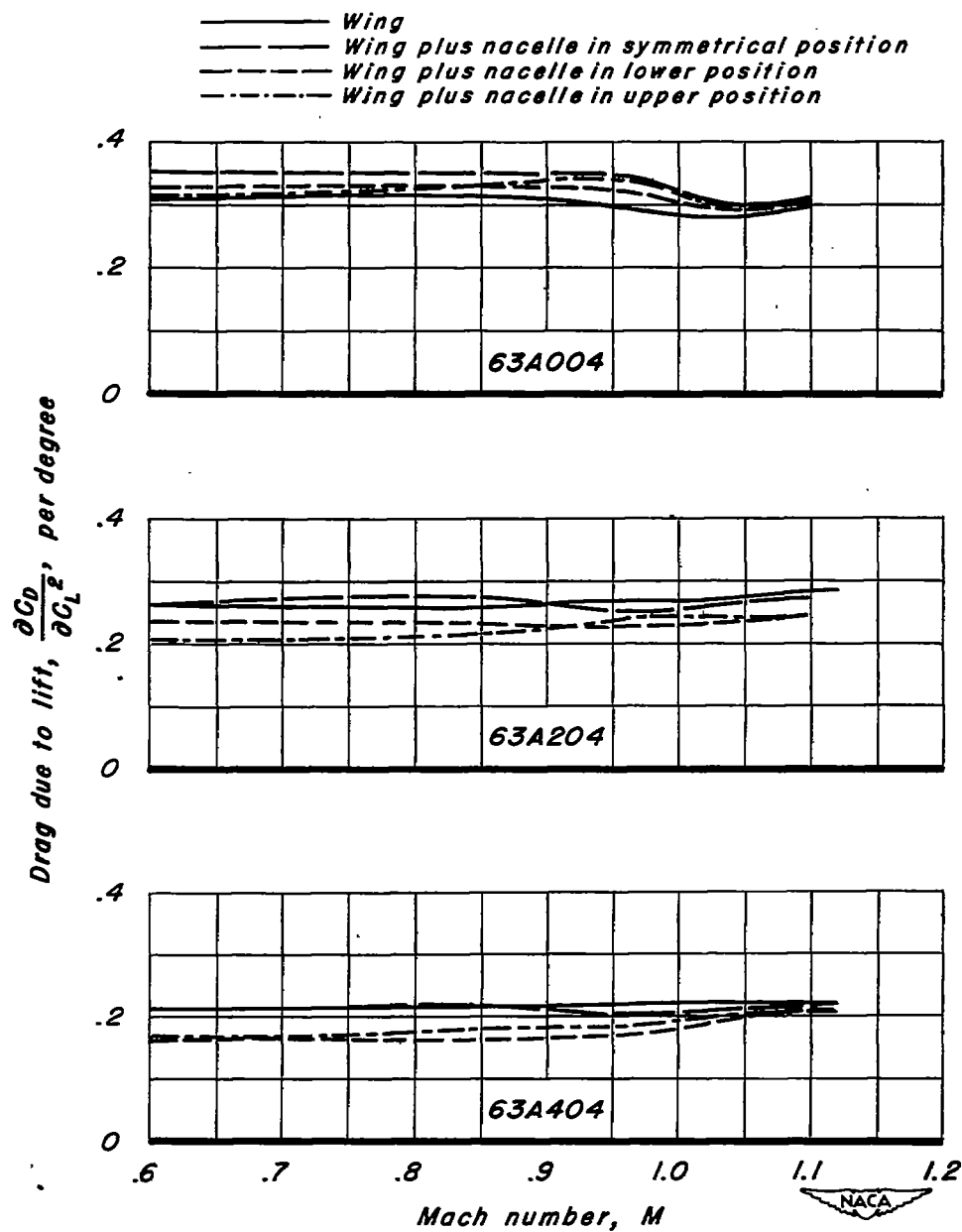
Wing
Wing plus nacelle in symmetrical position

63A004

63A204

63A404

Drag due to lift, $\frac{\partial C_D}{\partial C_L{}^2}$, per degree

Mach number, M

(d) A, 1.5; $\frac{t}{c}$, 0.04

Figure 11.— Continued.

Wing
——— Wing plus nacelle in symmetrical position
——— Wing plus nacelle in lower position
—·—·—·— Wing plus nacelle in upper position

(e) A, 2; $\frac{t}{c}$, 0.02

Figure II.— Continued.

Wing
Wing plus nacelle in symmetrical position
Wing plus nacelle in lower position
Wing plus nacelle in upper position

63A004

63A204

63A404

Mach number, M

(f) $A, 2;$ $\frac{t}{c}$, 0.04

Figure II.— Continued.

——————— Wing
——— · ——— Wing plus nacelle in symmetrical position
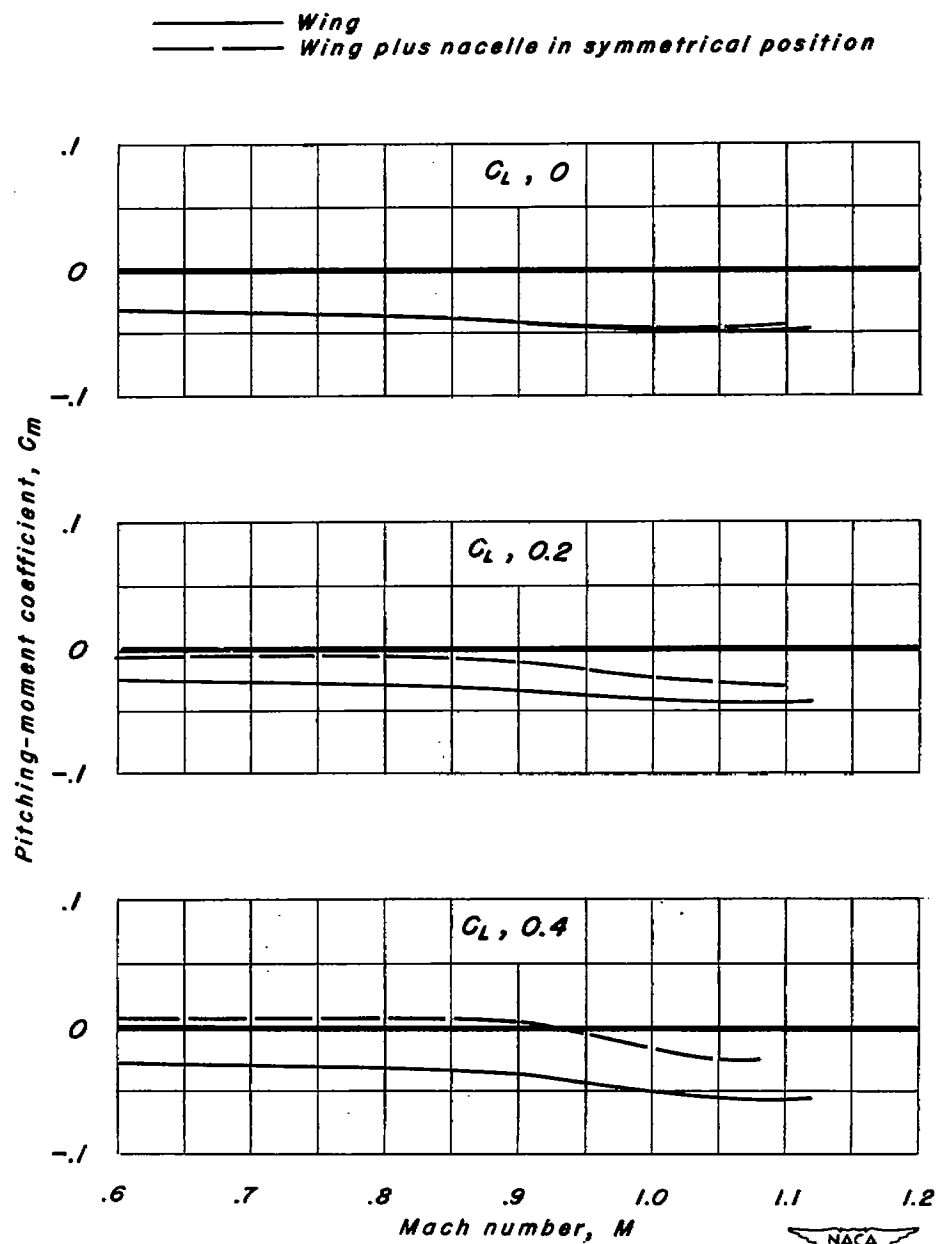— — — — Wing plus nacelle in lower position
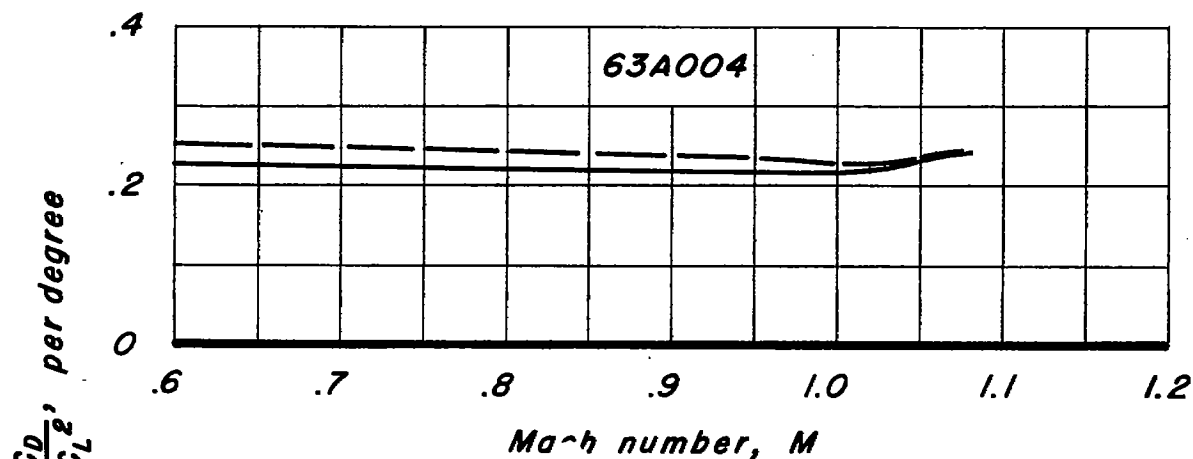
(g) A, 3; $\frac{t}{c}$, 0.04
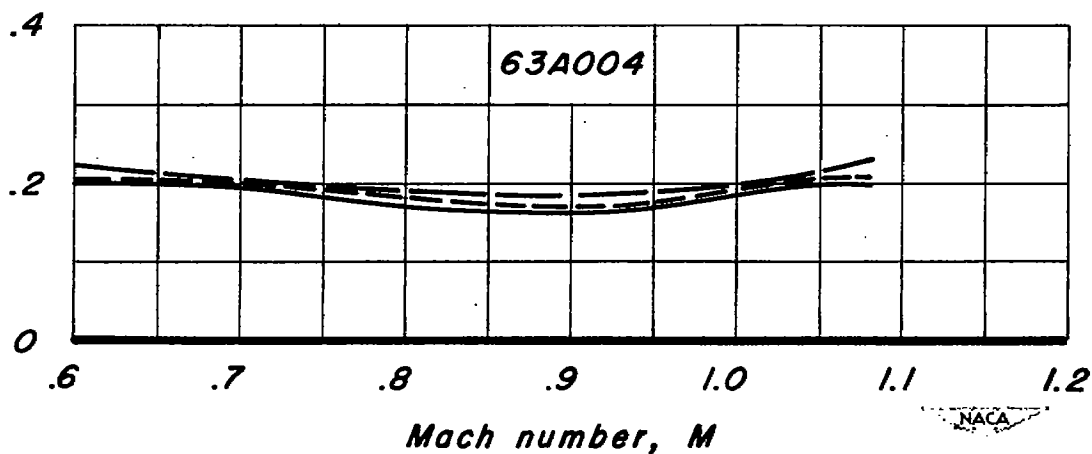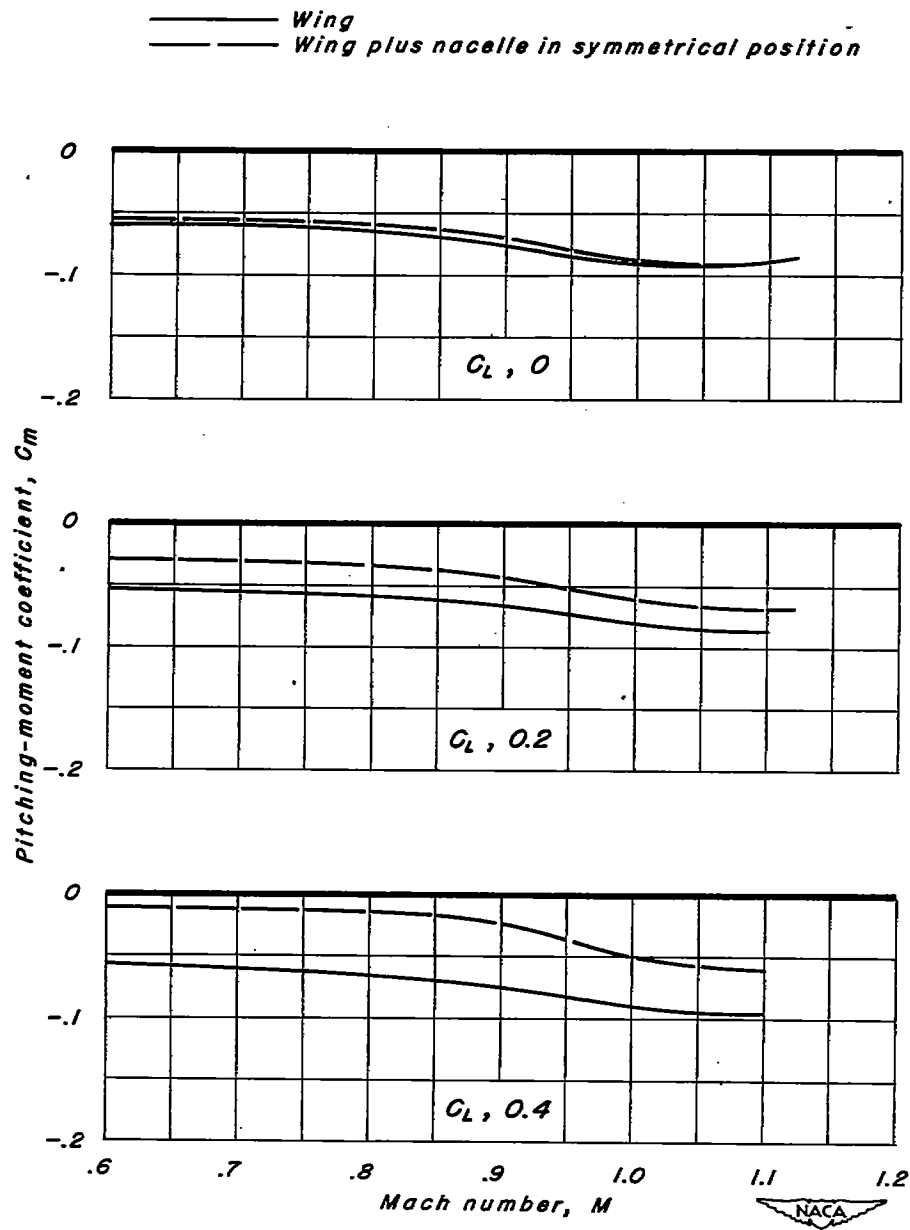

(h) A, 4; $\frac{t}{c}$, 0.04

Figure 11.—Concluded.
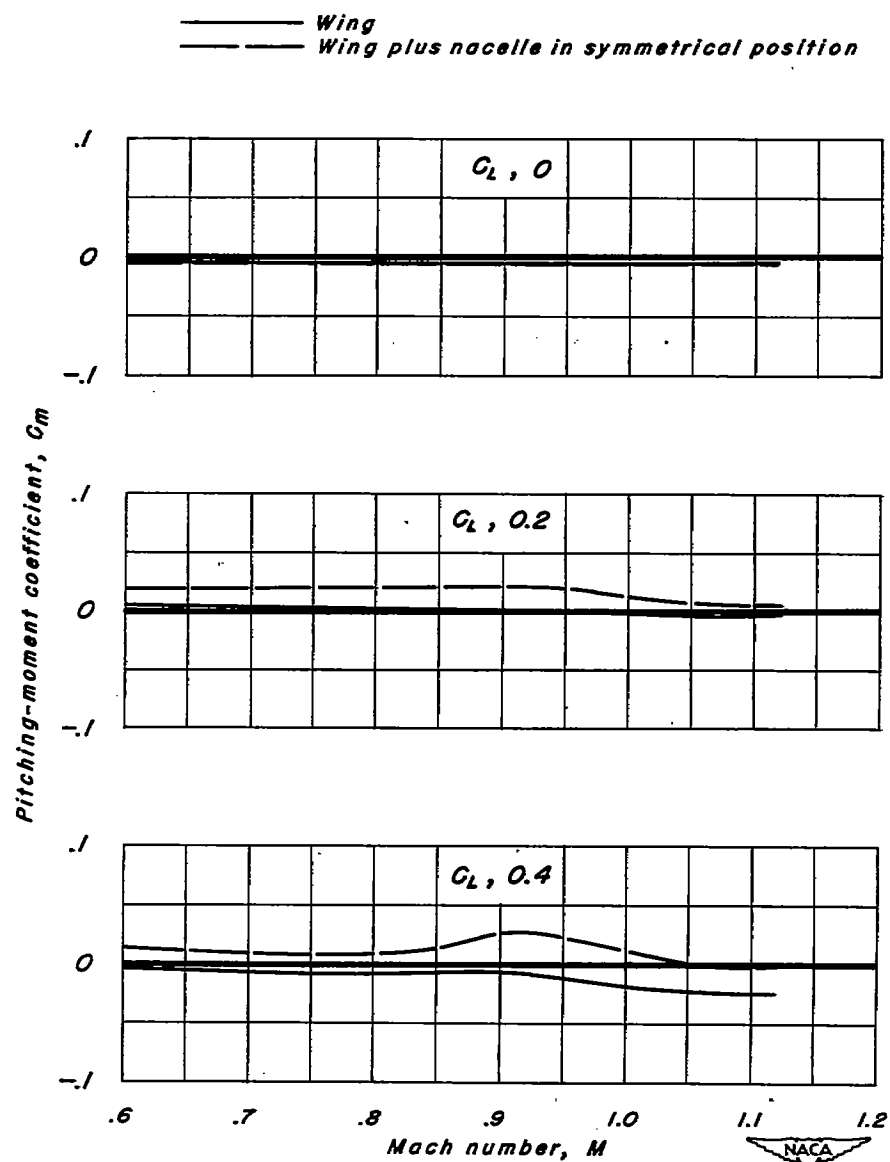
(a) A, 1; 63A002

Figure 12.-The variation of pitching-moment coefficient
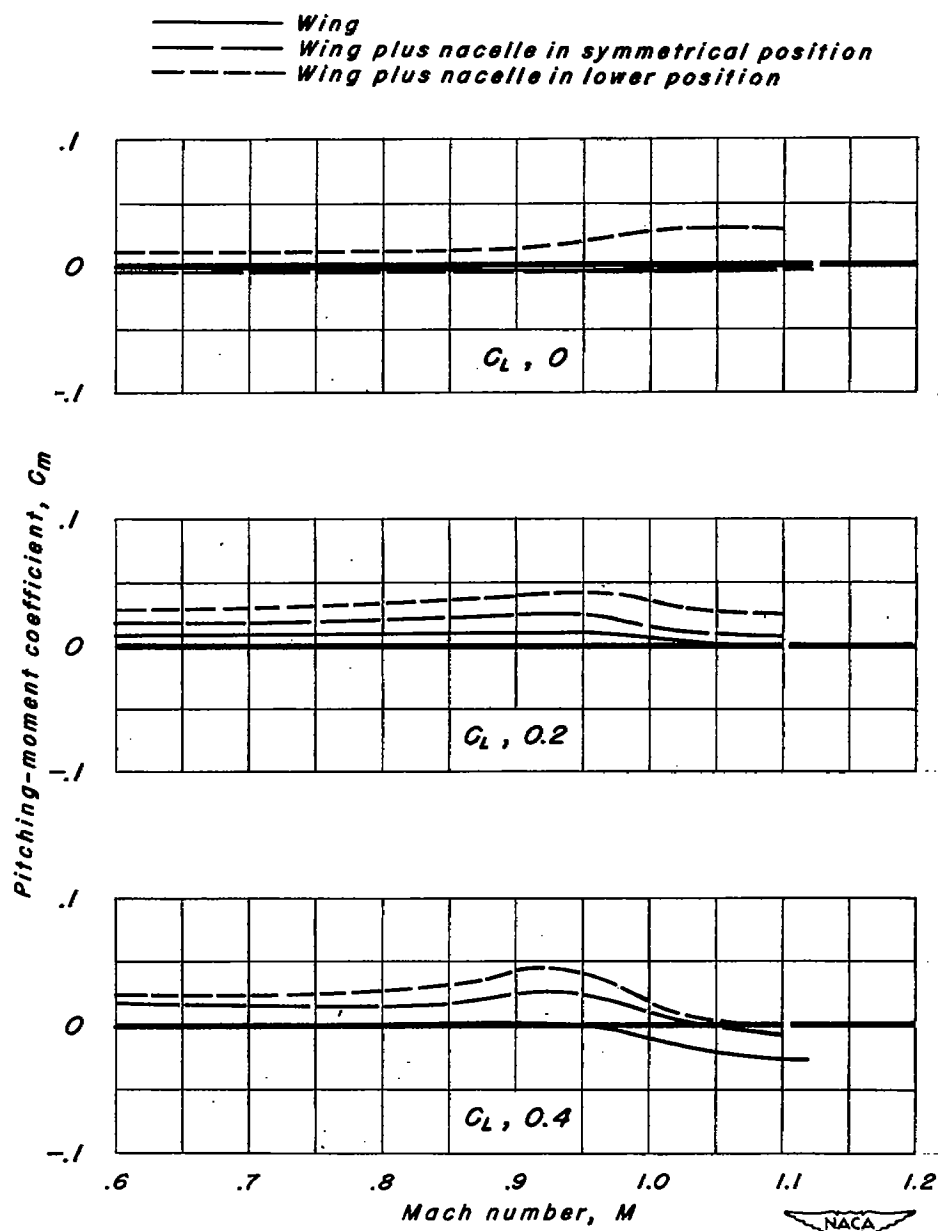with Mach number for the rectangular wings with
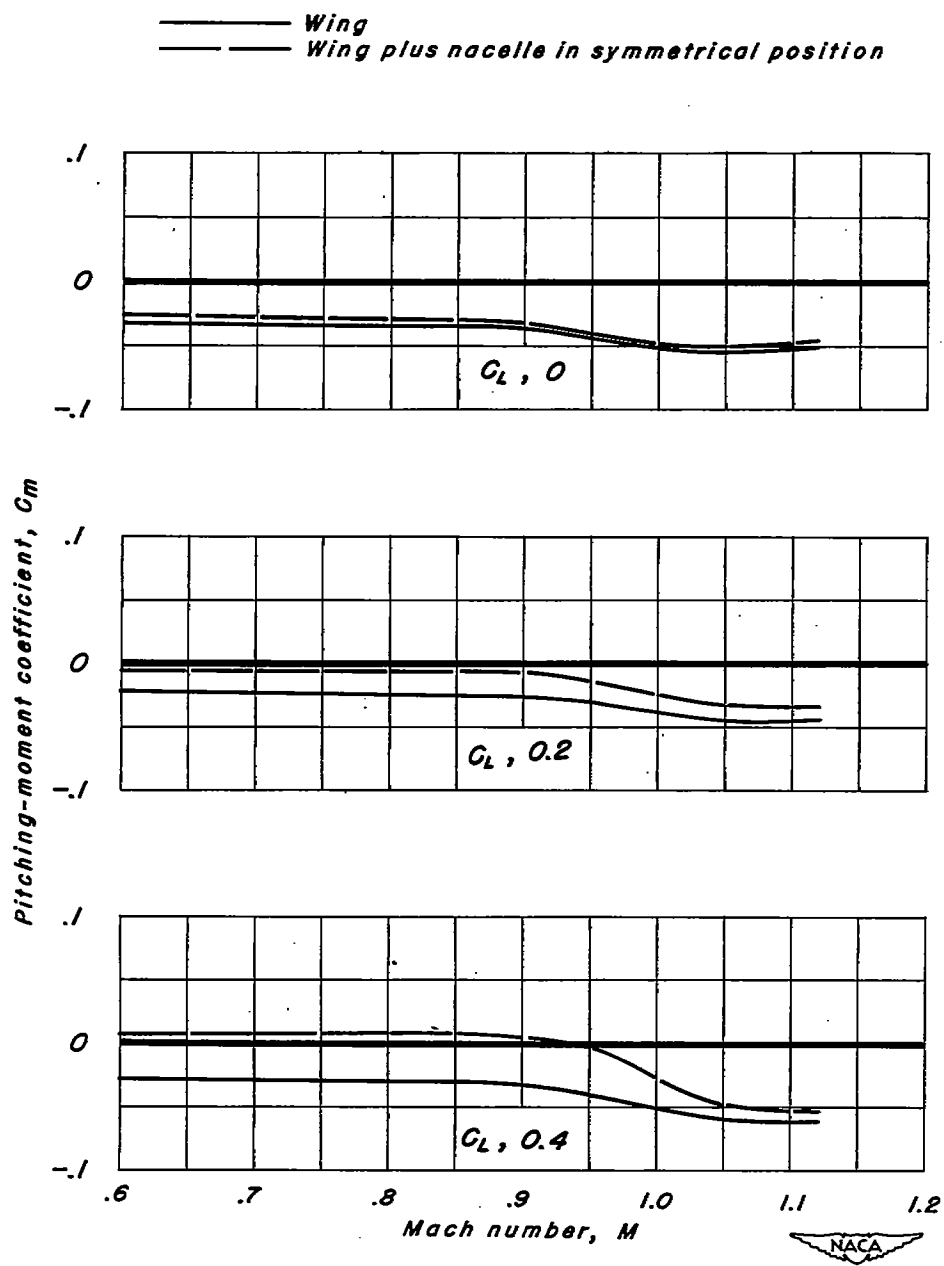NACA 63A series sections.

Wing
Wing plus nacelle in symmetrical position

(b) A, I ; 63A202

Figure 12.—Continued.

Wing
——— — Wing plus nacelle in symmetrical position

(c) A, 1 ; 63A402

Figure 12.—Continued.

Wing
Wing plus nacelle in symmetrical position
Wing plus nacelle in lower position

C_L, 0

C_L, 0.2

C_L, 0.4

Pitching-moment coefficient, C_m

Mach number, M

(d) A, l ; 63A004

Figure 12.-Continued.

Wing
Wing plus nacelle in symmetrical position

Pitching-moment coefficient, C_m

C_L , 0

C_L , 0.2

C_L , 0.4

Mach number, M

(e) A, I ; 63A204

Figure 12.—Continued.

—————— Wing
— — —— Wing plus nacelle in symmetrical position

(f) A, 1; 63A404

Figure 12.-Continued.

—————— Wing
———— —— Wing plus nacelle in symmetrical position

(g) A, 1.5; 63A002

Figure 12.- Continued.

——————— Wing
——— ——— Wing plus nacelle in symmetrical position

(h) A, 1.5; 63A202

Figure 12.- Continued.

Wing
Wing plus nacelle in symmetrical position

C_L , 0

C_L , 0.2

Pitching-moment coefficient, C_m

C_L , 0.4

Mach number, M

(i) A, 1.5; 63A402

Figure 12.- Continued.

Wing
Wing plus nacelle in symmetrical position

C_L, 0

C_L, 0.2

C_L, 0.4

Pitching-moment coefficient, C_m

Mach number, M

(j) A, 1.5; 63A004

Figure 12.- Continued.

Wing
Wing plus nacelle in symmetrical position

C_L , 0

C_L , 0.2

C_L , 0.4

Mach number, M

Pitching-moment coefficient, C_m

(k) A, 1.5; 63A204

Figure 12.-Continued.

Wing
Wing plus nacelle in symmetrical position

C_L , 0

C_L , 0.2

C_L , 0.4

Pitching-moment coefficient, C_m

Mach number, M

(l) A, 1.5; 63A404

Figure 12.-Continued.

Wing
Wing plus nacelle in symmetrical position
Wing plus nacelle in lower position
Wing plus nacelle in upper position

C_L , 0

C_L , 0.2

C_L , 0.4

Pitching-moment coefficient, C_m

Mach number, M

(m) A, 2 ; 63A002

Figure 12.-Continued.

Wing
Wing plus nacelle in symmetrical position
Wing plus nacelle in lower position
Wing plus nacelle in upper position

C_L , 0

C_L , 0.2

C_L , 0.4

Pitching-moment coefficient, C_m

Mach number, M

(n) A, 2; 63A202

Figure 12.- Continued.

Wing
Wing plus nacelle in symmetrical position
Wing plus nacelle in lower position
Wing plus nacelle in upper position

C_L , 0

C_L , 0.2

C_L , 0.4

Pitching-moment coefficient, C_m

Mach number, M

(o) A, 2; 63A402

Figure 12.- Continued.

Wing
—————— Wing plus nacelle in symmetrical position
— — — Wing plus nacelle in lower position
—·——·—— Wing plus nacelle in upper position

C_L, 0

C_L, 0.2

C_L, 0.4

Pitching-moment coefficient, C_m

Mach number, M

(p) A, 2; 63A004

Figure 12.- Continued.

———— Wing
—— —— Wing plus nacelle in symmetrical position
— — — Wing plus nacelle in lower position
—·—··—·— Wing plus nacelle in upper position

C_L , 0

C_L , 0.2

C_L , 0.4

Pitching-moment coefficient, C_m

Mach number, M

(q) A,2; 63A204

Figure 12.– Continued.

(r) A,2; 63A404

Figure 12.-Continued.

Wing
Wing plus nacelle in symmetrical position

C_L, 0

C_L, 0.2

C_L, 0.4

Pitching-moment coefficient, C_m

Mach number, M

(s) A, 3; 63A004

Figure 12.- Continued.

Wing
Wing plus nacelle in symmetrical position
Wing plus nacelle in lower position
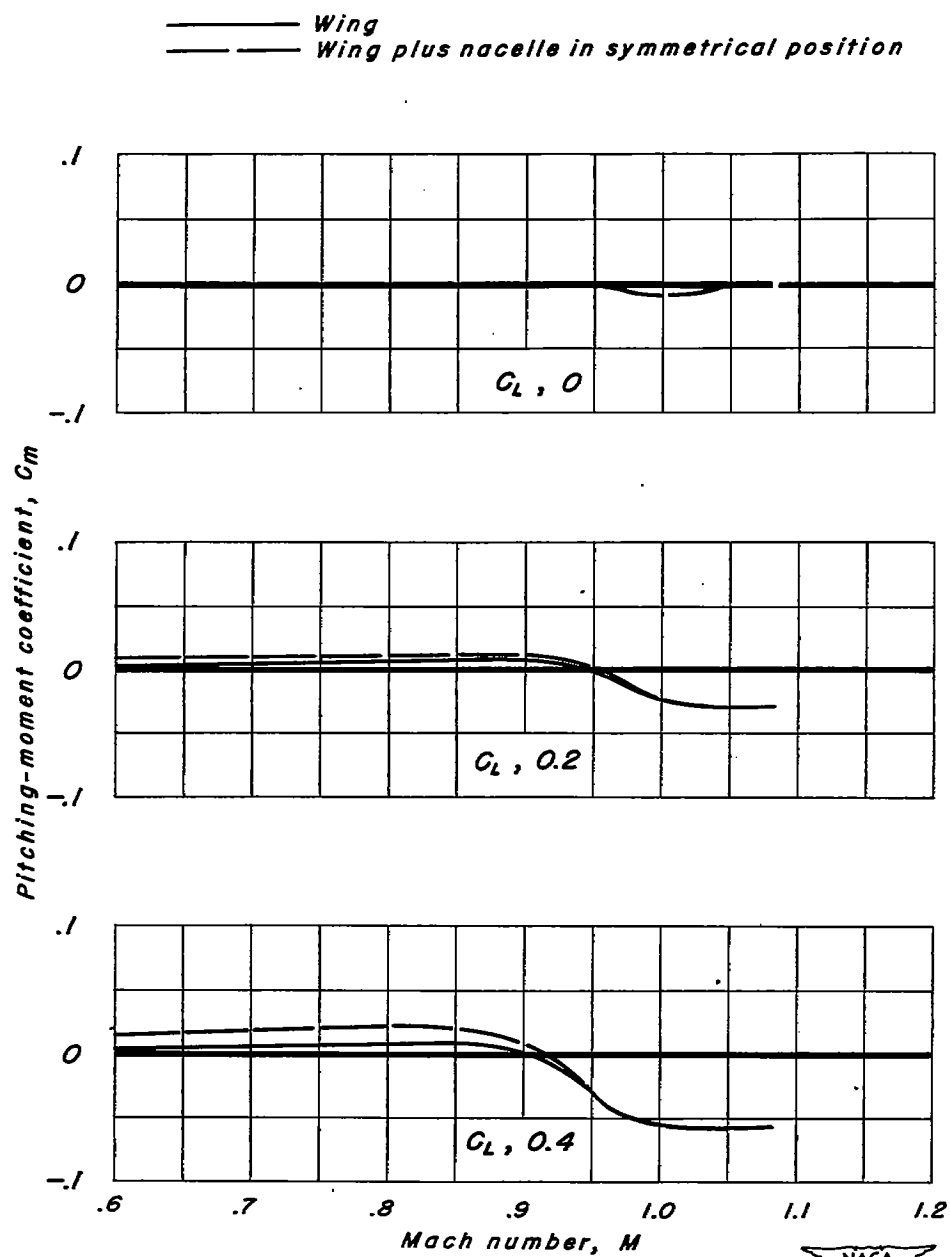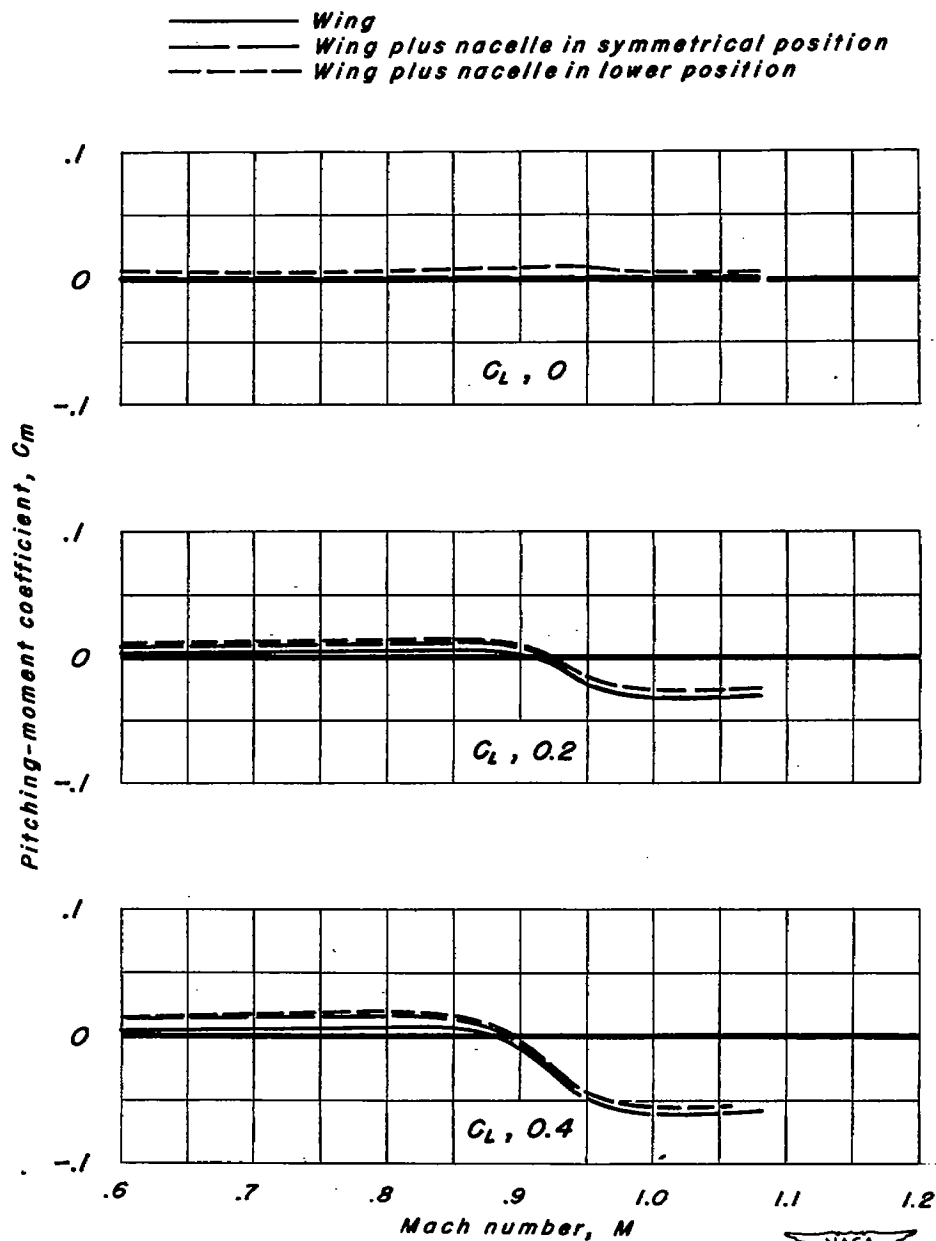
(t) A, 4; 63A004

Figure 12.- Concluded.
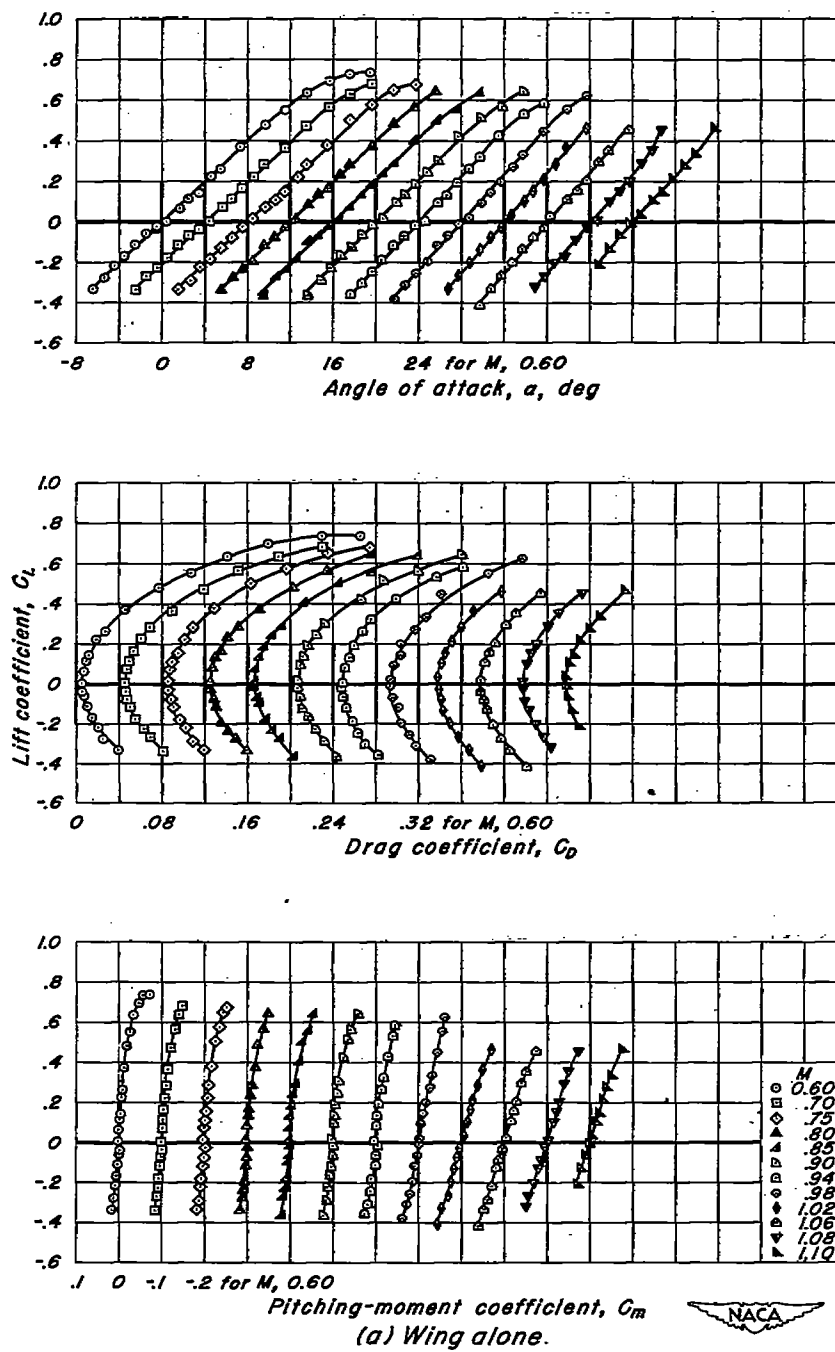
Figure 13.—The aerodynamic characteristics of the tapered wing.

(b) Wing plus nacelle in symmetrical position.
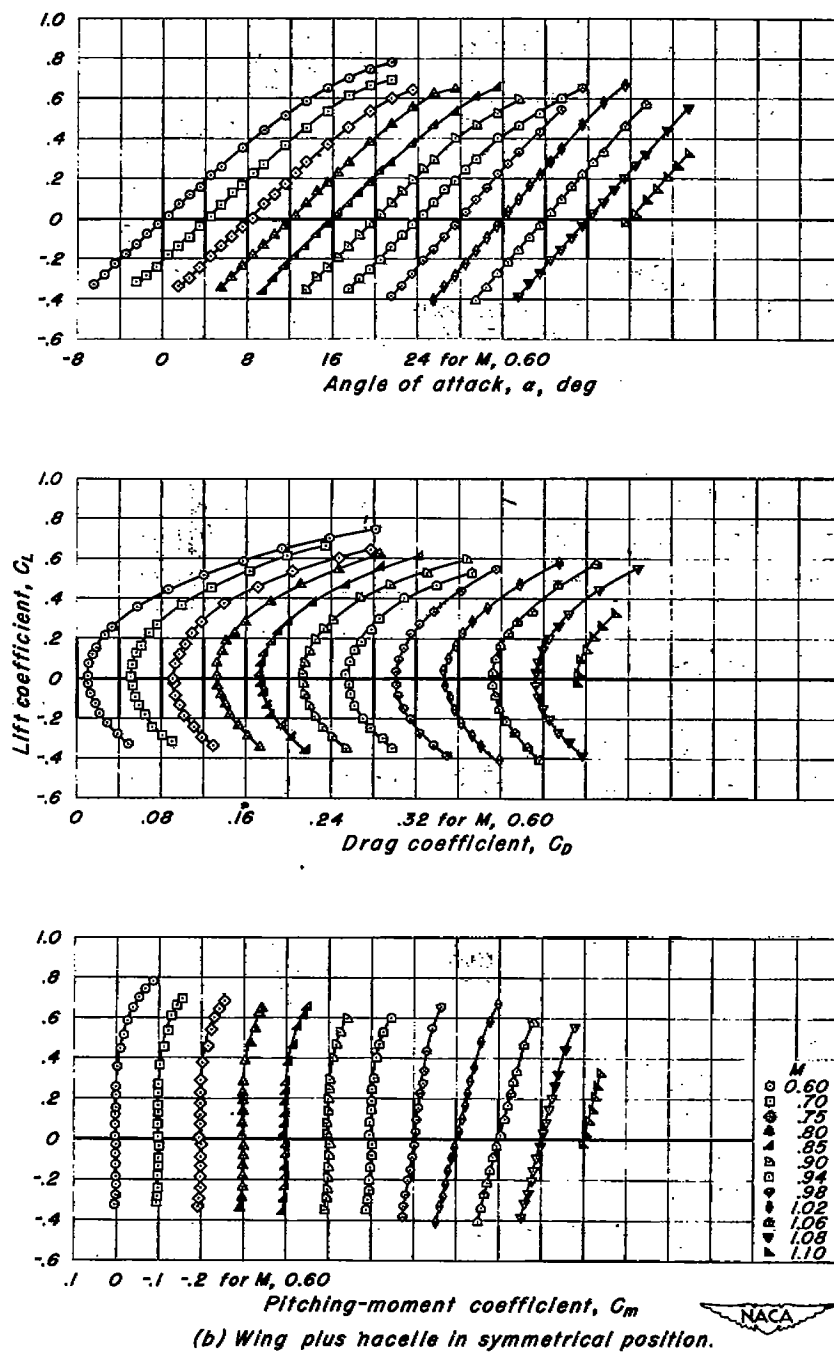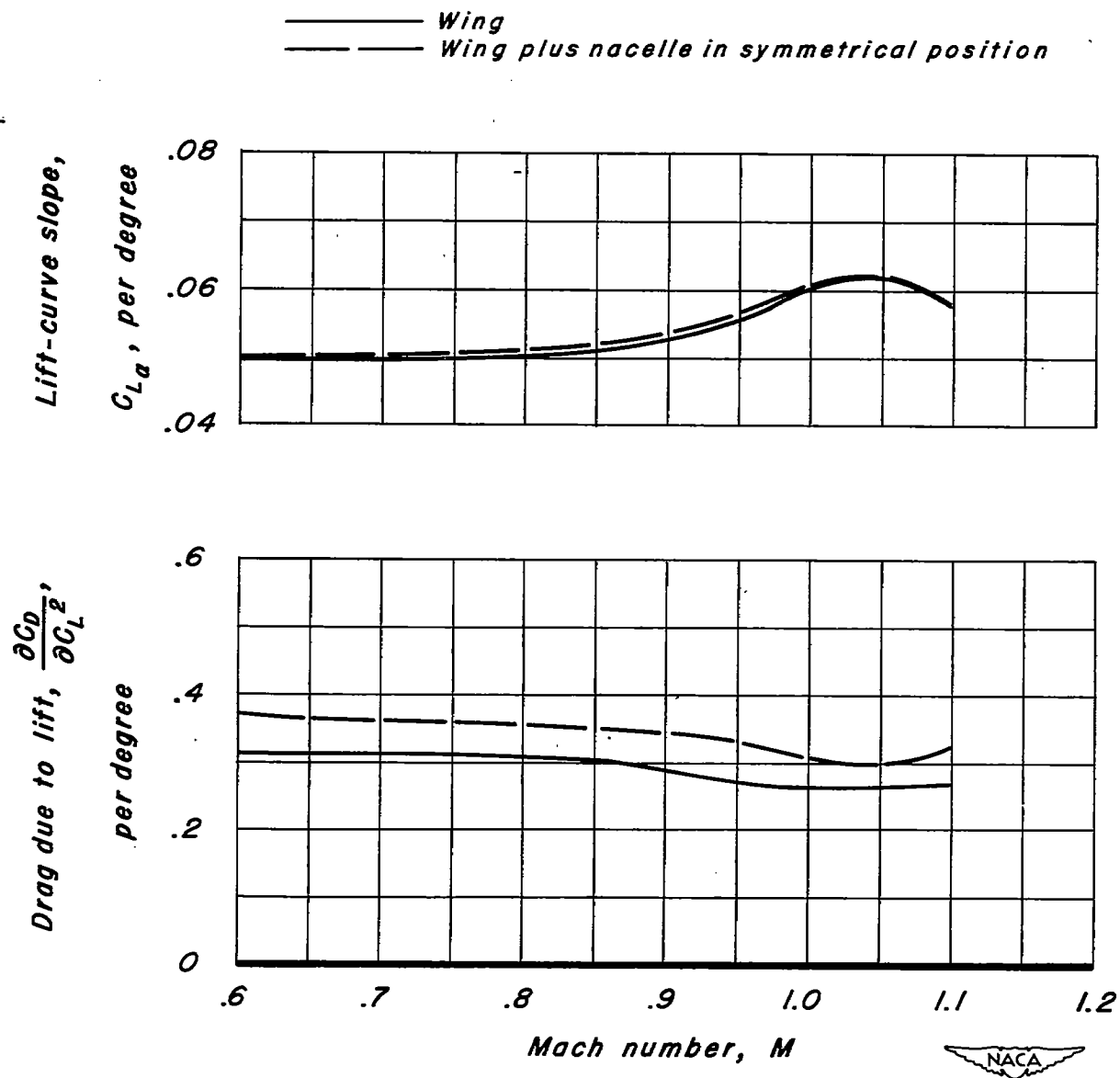
Figure 13.—Concluded.

Wing
Wing plus nacelle in symmetrical position

Figure 14.—The variation with Mach number of the parameters C_{L_α} and $\partial C_D / \partial C_L^2$ for the tapered wing.

——————— Wing
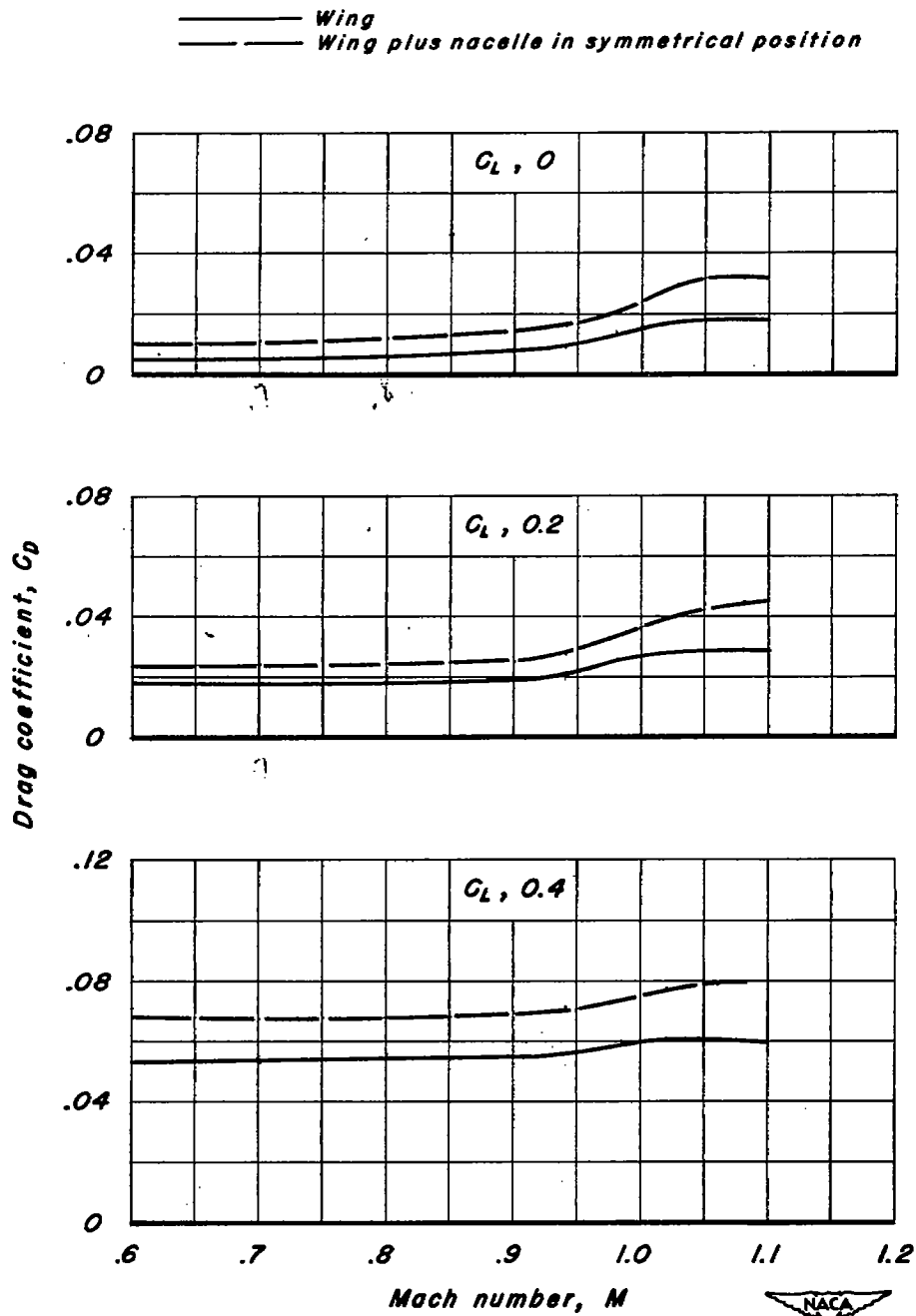——— · ——— Wing plus nacelle in symmetrical position

Figure 15.—The variation of drag coefficient with Mach
number for the tapered wing.

——————— Wing
— — — Wing plus nacelle in symmetrical position

C_L , 0

C_L , 0.2

C_L , 0.4

.6   .7   .8   .9   1.0   1.1   1.2
Mach number, M

Pitching-moment coefficient, C_m
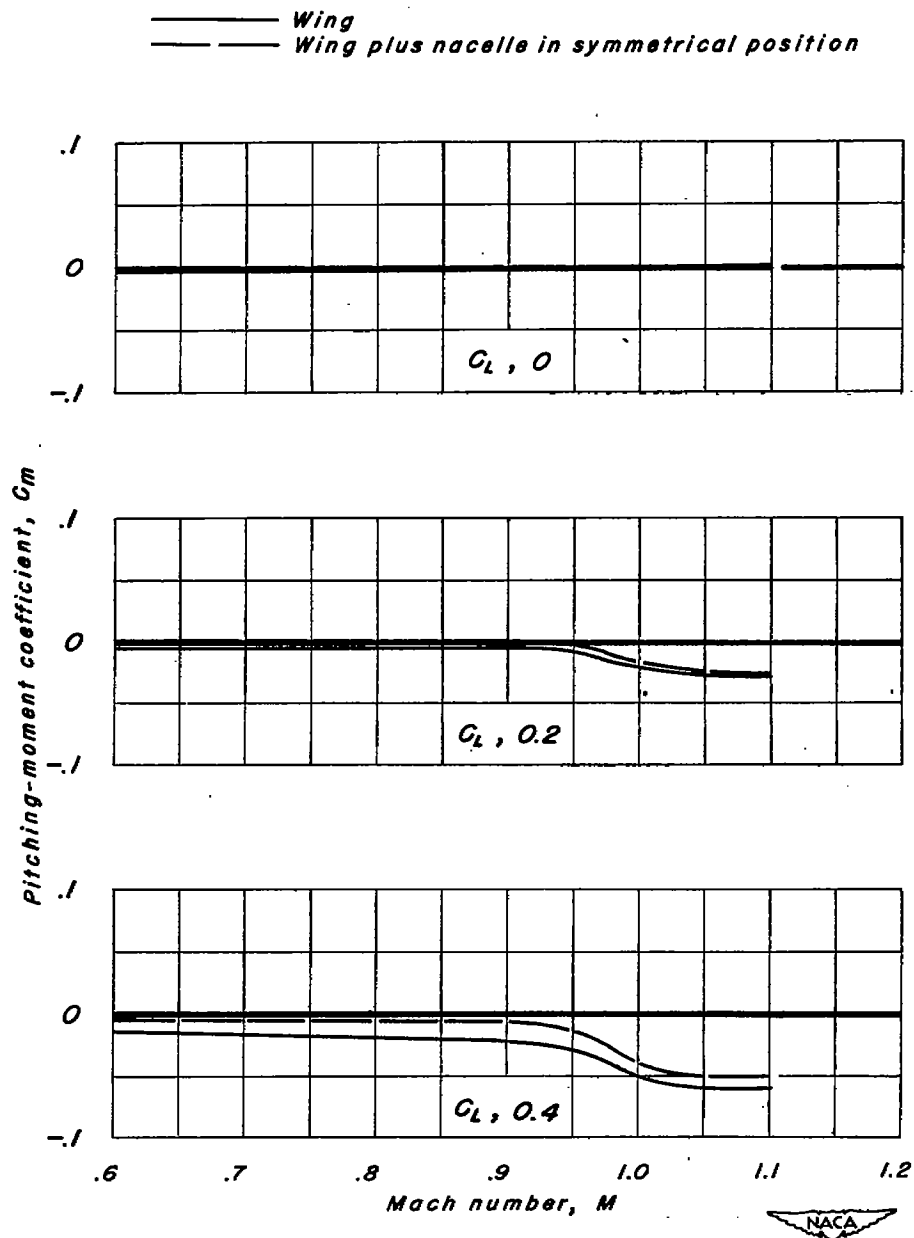
Figure 16.—The variation of pitching-moment coefficient
with Mach number for the tapered wing.

DO NOT REMOVE SLIP FROM MATERIAL

Delete your name from this slip when returning material to the library.

NAME	MS
Sudaram	9/2

NASA Langley (Rev. May 1988)   RIAD N-75